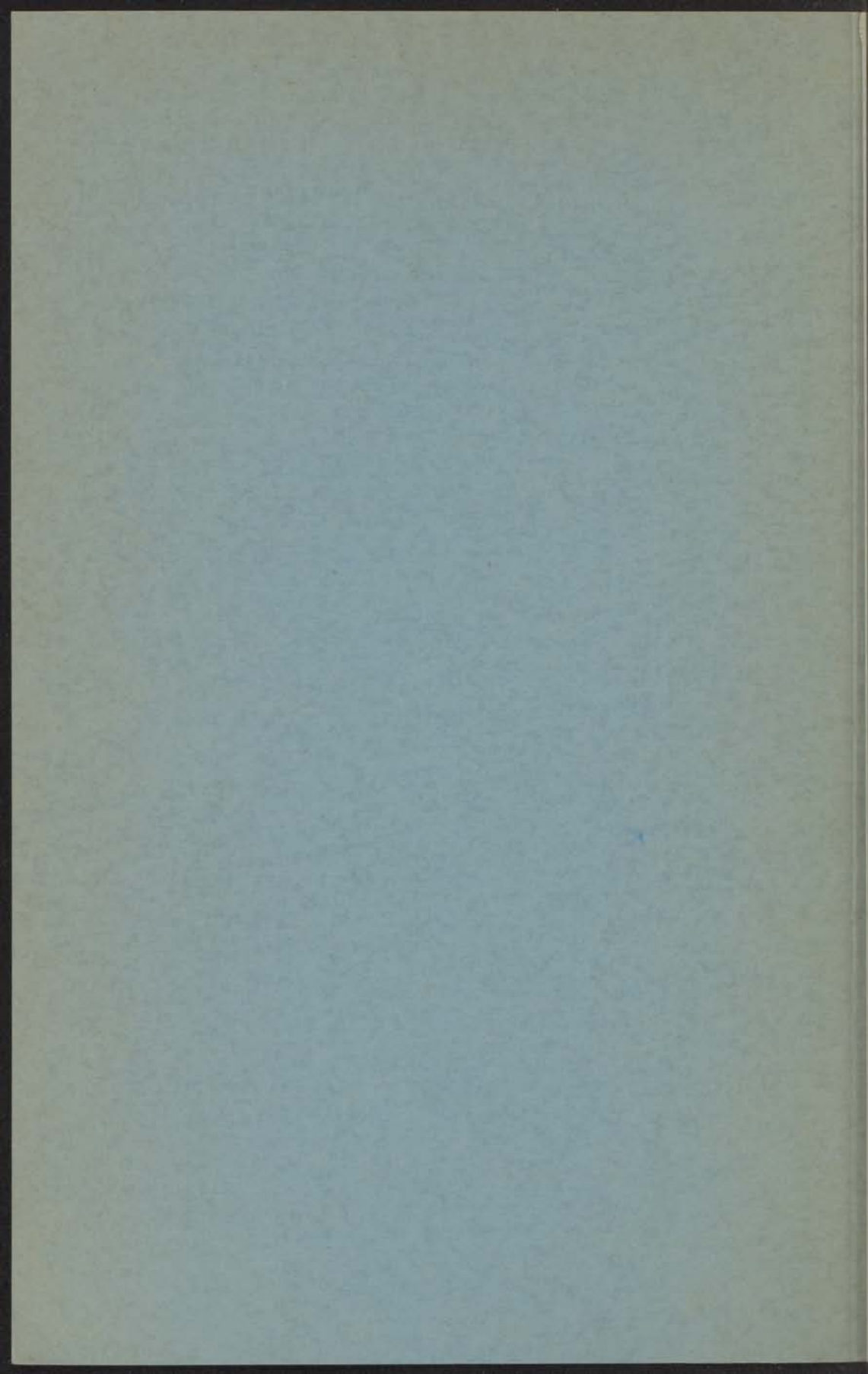


12 JUNI 1972

SOME ASPECTS OF ION-ATOM AND ION-MOLECULE COLLISIONS

INSTITUUT-LORIENTE
van de technische universiteit
Nieuwegein 10-Londen-Medische

H. VAN DOP

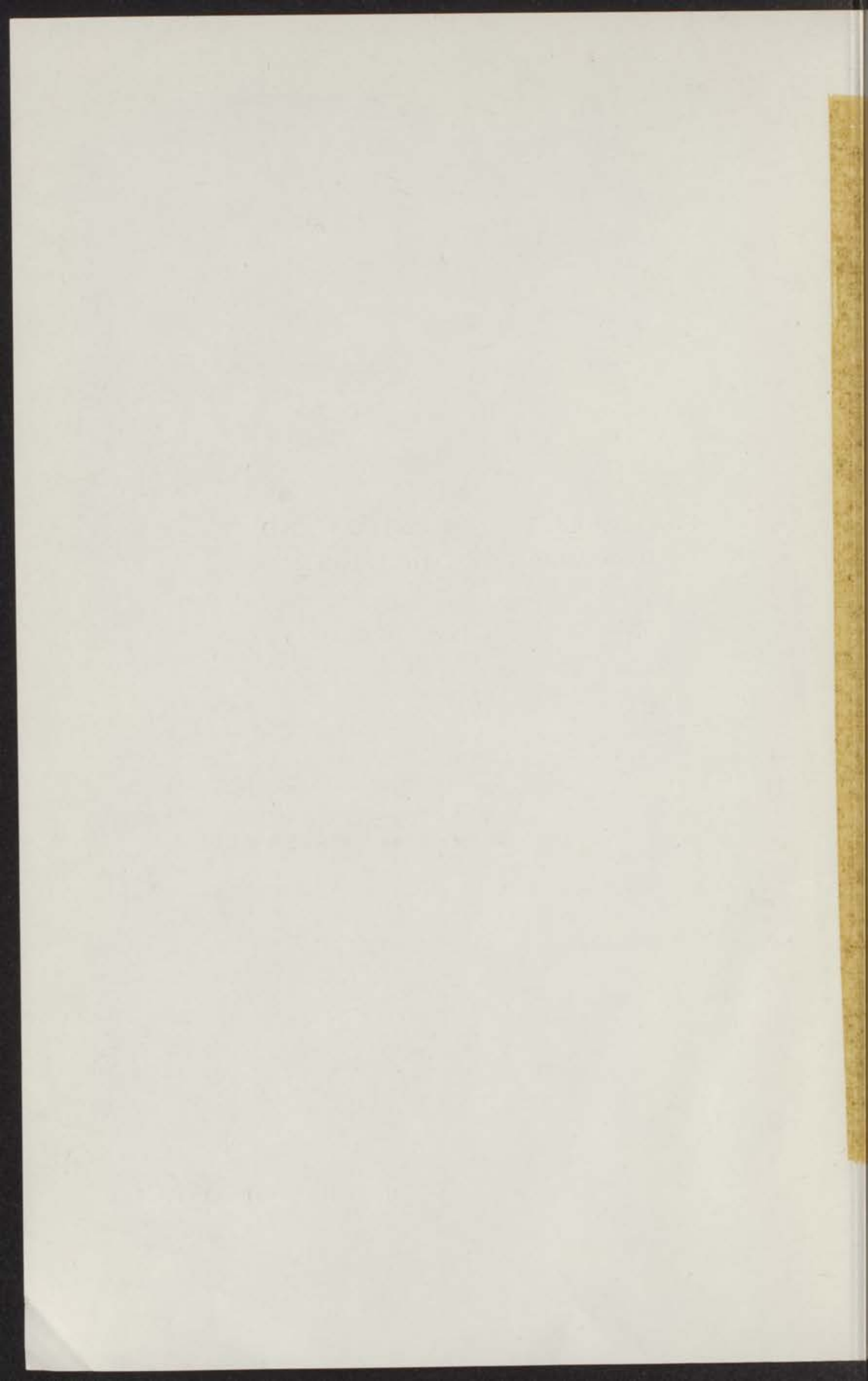


12 JUNI 1972

SOME ASPECTS OF ION-ATOM AND
ION-MOLECULE COLLISIONS

INSTITUUT-LORENTZ
voor theoretische natuurkunde
Nieuwsteeg 18-Leiden-Nederland

kast dissertaties



STELLINGEN

I

Voor de bepaling van de wisselwerkingspotentiaal heeft het meten van elastische botsingsdoorsneden, als functie van de hoek, bepaalde voordelen boven het meten van deze doorsneden als functie van de energie volgens de methode van Amdur.

Jordan, J. E., Amdur, I., *J. Chem. Phys.* **46** (1967) 165.

II

De verschillen tussen elastische botsingsdoorsneden van de combinaties Ar-H₂ en Ar-D₂ zijn te groot om geheel aan de bijdrage van terugwaartse verstrooiing te kunnen worden toegeschreven.

Jordan, J. E., Amdur, I., *J. Chem. Phys.* **46** (1967) 4145.

III

De verschillen die bij dezelfde energie optreden tussen centrale botsingen van kalium-, respectievelijk lithium-ionen met het molecuul waterstof, kunnen eenvoudig worden verklaard door het verschil in het standaardgetal, $\alpha = \lambda^2 A / kL^2$.

Dit proefschrift, laatste hoofdstuk.

IV

Een gebruikelijke techniek bij het schoonmaken van oppervlakken in vacuümsystemen is uitstoken. Het is echter niet triviaal dat bij verhitting van een oppervlak de bedekkingsgraad zal afnemen.

M. Kaminsky, *Atomic and Ionic Impact Phenomena on Metal Surfaces XXV*, Springer Verlag (Berlijn, Heidelberg, New York, 1965).

Logan, A. M., Keck, J. C., *J. Chem. Phys.* **49** (1968) 860.

V

Een bovengrens voor de levensduur van aangeslagen toestanden in hooggeïoniseerde atomen kan worden bepaald uit de verzwakking van de γ -hoek correlatie ten gevolge van de desoriëntatie van de kernspin.

Berant *et al.*, *Z., Nucl. Phys. A* **178** (1971) 155.

VI

De toepassing van een channelplate in hoekafhankelijke verstrooiings-experimenten biedt goede perspectieven.

IEEE Trans. Nucl. Sci. 17-3 (1970) 367.

VII

Baede geeft een model dat de kwalitatieve verschillen in de energie-afhankelijkheid van de werkzame doorsneden voor atoom-ion vorming bij de reacties van J_2 met respectievelijk K en Na verklaart. Er wordt geen rekening gehouden met de mogelijkheid tot molecuul-ion vorming.

Het uit dit model volgende gedrag wordt hierdoor echter niet aangetast, aangenomen dat de molecuul-ion fractie een constante is.

A. P. M. Baede, proefschrift (Amsterdam, 1972).

VIII

Van der Schroeff maakt ten onrechte een onderscheid tussen de door hem geïntroduceerde begrippen isochroon en chronoquant en de in de literatuur gebruikelijke begrippen productcurve en isoquant.

H. J. van der Schroeff, *Kwantitatieve verhoudingen, kosten en economische proportionaliteit*, 2e druk, Kosmos (Amsterdam, Antwerpen, 1967).

IX

Het "life detection" experiment dat in het kader van het Viking project op de planeet Mars zal worden uitgevoerd is onnodig gecompliceerd.

1973 Viking voyage to Mars. Viking Project Management, 1969 Astronaut **7**, 30.

X

De scepsis in Nabokov's "Ada" ten aanzien van enkele consequenties van de speciale relativiteitstheorie berust op verdachtmakingen en foutieve interpretaties.

V. Nabokov, *Ada*, Penguin Books Ltd. (Harmondsworth, 1970).

XI

Nederland heeft de twijfelachtige eer het – aan Heine toegeschreven – enigszins denigrerende gezegde: "Als de wereld vergaat ga ik naar Nederland, want daar gebeurt toch alles vijftig jaar later", waarschijnlijk weerlegd te zien door een rapport samengesteld in opdracht van de club van Rome.

Rapport van de club van Rome, Het Spectrum (Utrecht, Arnhem, 1972).

Leiden, 22 juni 1972.

H. VAN DOP

... van de ...
 ... van de ...
 ... van de ...

... van de ...
 ... van de ...
 ... van de ...

... van de ...

... van de ...
 ... van de ...
 ... van de ...

... van de ...

A. P. K. ... (Amsterdam, 1977)

... van de ...
 ... van de ...
 ... van de ...

H. J. van ... (Amsterdam, 1977)

... van de ...
 ... van de ...
 ... van de ...

H. J. van ... (Amsterdam, 1977)

SOME ASPECTS OF ION-ATOM AND ION-MOLECULE COLLISIONS

PROEFSCHRIFT

TER VERKRIJGING VAN DE GRAAD VAN DOCTOR IN
DE WISKUNDE EN NATUURWETENSCHAPPEN AAN
DE RIJKSUNIVERSITEIT TE LEIDEN, OP GEZAG VAN
DE RECTOR MAGNIFICUS DR. W. R. O. GOSLINGS,
HOGLERAAR IN DE FACULTEIT DER GENEESKUNDE,
VOLGENS BESLUIT VAN HET COLLEGE VAN DEKANEN
TE VERDEDIGEN OP DONDERDAG 22 JUNI 1972
TE KLOKKE 16.15 UUR

DOOR

HENDRICUS VAN DOP
GEBOREN TE ZUILEN IN 1944

SOME ASPECTS OF ION-ATOM AND ION-MOLECULE COLLISIONS

PROEFTSCHRIFT

THE TERRITORY OF THE GREAT THE DOCTOR IN
BY WILHELMUS HATERWYTERSCHEPPE VAN
ON UNIVERSITEIT IN THE OF GREAT VAN
DE KUNSTEN WAKINGEN DE W. H. B. COLLEGE
WOLLEBAAN IN DE TACHTSTAD OOR DEN KUNSTEN
WOLLEBAAN DEELT EENIGE TOEGE TOEGE
IN DE VERBODENEN DE WOLLEBAAN IN DEELT
DE KUNSTEN WAKINGEN

Promotor: PROF. DR. J. LOS

1968

HERENICE VAN DOT

GEBOREN IN JULIJ 1944

CONTENTS

I INTRODUCTION

II COLLECTED PAPERS

1. Theorie begroting of positieve en negatieve verandering in het
Lorentz-factor (relativiteitstheorie).
Physica 24 (1957) 227-244.
2. Theorie begroting of de "classieke" theorie van de positieve en negatieve
verandering in het Lorentz-factor.
To be published in Physica.
Thesis (1957) 1-4.
3. Theorie begroting of verandering in het Lorentz-factor (relativiteitstheorie).
To be published in Physica.
Thesis (1957) 1-4.
4. Theorie begroting of verandering in het Lorentz-factor (relativiteitstheorie).
Thesis (1957) 227-244.
5. Theorie begroting of verandering in het Lorentz-factor (relativiteitstheorie).
To be published in Physica.
Thesis (1957) 1-4.

III SUMMARY

IV CURRICULUM VITAE

*Aan Jolijn
Aan mijn ouders*

PROF. DR. J. K. K.

1911

CONTENTS

I INTRODUCTION

II COLLECTED PAPERS

1. Elastic scattering of particles with noble gas electron configuration in the energy range from 150 through 4000 eV.
Physica 46 (1970) 458-468.
2. Elastic scattering of K^+ -ions from diatomic molecules in the energy range from 150 to 4000 eV.
To be published in *Physica*.
Physica 247 (1972) 1-4
3. The semi classical equivalence in the case of non spherical scattering.
To be published in *Physica*.
Physica 188 (1972) 1-9
4. Energy loss measurements of K^+ -ions in head-on collisions with He, H_2 and D_2 .
Physica 54 (1971) 223-236.
5. Calculations on energy transfer to a diatomic molecule in high energy head-on collisions.
To be published in *Physica*.
Physica 202 (1972) 1-10

III SUMMARY

IV CURRICULUM VITAE

CONTENTS

I INTRODUCTION

II COLLECTED PAPERS

1. Some constants of particles with mass and electric charge in the
field of a point charge (S. G. Gerasimov)
Pages 1-10
2. Some constants of particles with mass and electric charge in the
field of a point charge (S. G. Gerasimov)
To be published in Physics
Pages 1-10
3. The movement of particles in the field of a point charge
To be published in Physics
Pages 1-10
4. Some constants of particles with mass and electric charge in the
field of a point charge (S. G. Gerasimov)
Pages 1-10
5. Some constants of particles with mass and electric charge in the
field of a point charge (S. G. Gerasimov)
To be published in Physics
Pages 1-10

III SUMMARY

IV BIBLIOGRAPHY

INTRODUCTION

The papers presented in this thesis give an account of the investigation into ion-atom and ion-molecule collisions. The data on elastic scattering are an extension of the work of Amdur and they concern the experimental determination of (repulsive) forces between particles eventually with internal structure (atoms and molecules). The experimental data are obtained by letting an ion beam pass a collision chamber which is filled with some gas. The attenuation of the ion beam – which is caused by collisions, such that the ions are scattered over an angle larger than a fixed apparatus angle contains information about the forces during the interaction. As it is in general not possible to convert the experimental data directly into an interaction potential, one usually chooses a potential model. From the fit to the experimental data, it is possible to determine the potential parameters. In the first paper this procedure is followed to determine interaction potentials between potassium and chlorine ions on the one side and rare gas atoms on the other.

In the second paper ion-molecule potential parameters are determined. In this case the assumption is made that the total interaction is a sum of pairwise ion-atom interactions. As a consequence the scattering is dependent on the orientation of the molecule with respect to the incident direction. As in the actual experiment the target molecules have random orientations the cross-sections will be averaged so that the resulting ion-molecule potential is an average of the angular dependant two-centre potential. A consequence of this model is that it introduces small differences in cross-section for collisions with homo- and heteronuclear isotopic molecules. An attempt to measure these effects has failed. It has led, however, to some general considerations concerning angular dependent scattering: It is well known that under certain conditions the quantum mechanical description of scattering phenomenae changes over to the classical description. The conditions under which quantum mechanical expressions reduce to classical ones are discussed in the third paper, and applied to non-spherical scattering.

Finally some inelastic processes occurring in ion-molecule collisions have

been investigated. By means of energy analysis of the scattered ions it is possible to determine inelastic energy losses. In these kind of collisions the molecule is excited into higher vibrational states or - at higher collision energy - into the continuum. The fourth paper contains the experimental results of energy loss measurements for potassium ions incident on hydrogen and deuterium molecules.

In the last paper an attempt is made to give a theoretical description of these inelastic ion-molecule collisions. For this purpose a collision model was constructed on which classical trajectory calculations are performed.

ELASTIC SCATTERING OF PARTICLES WITH NOBLE GAS ELECTRON CONFIGURATION IN THE ENERGY RANGE FROM 150 THROUGH 4000 eV

A. J. H. BOERBOOM, H. VAN DOP and J. LOS
FOM-Instituut voor Atoom- en Molecuulfysica, Amsterdam

Received 7 July 1969

Dedicated to Professor Dr. I. Amdur on the occasion of his 60th birthday,
January 24, 1970.

Synopsis

Integral cross sections for elastic scattering of K^+ and Cl^- ions *vs.* noble gas atoms (He, Ne, Ar, Kr, Xe) were determined respectively in the energy range from 150 through 4000 and from 2400 through 4000 eV. This was done by shooting a well confined K^+ or Cl^- beam through a collision chamber filled with the target gas.

From these cross section measurements we deduced the interaction potentials. We have used three potential models: the inverse power model $V(r) = K/r^s$, the exponential model $V(r) = A e^{-\alpha r}$ and the screened Coulomb model $V(r) = (C/r) e^{-r/a}$. The exponential model and the Coulomb model fitted very well, and over a large range of internuclear separations. The inverse power model was only valid in small ranges and is less satisfying than the other two models. Moreover, we could establish qualitatively the relative contraction of the K^+ ion with respect to the Cl^- ion.

Finally we have made a comparison between our measurements and other theoretical and experimental data. The agreement with the experiments of Amdur *et al.* was satisfactory but there is some discrepancy with theoretical *ab initio* calculations.

1. *Introduction.* In continuation of our K^+ -Ar collision cross section measurements¹⁾, we also measured the collision cross sections of K^+ with other noble gas atoms. The K^+ -Ar experiment was originally done to compare the results with the Ar *vs.* Ar measurements of I. Amdur *et al.*¹⁾. We have now extended the measurements to other noble gas atoms. To complete the experiments we also investigated the Cl^- -noble gas interaction, as the Cl^- ion has the same electronic structure as the K^+ ion and the Ar atom.

From the cross sections we deduced some interaction potentials and their respective ranges of validity.

2. *Experimental.* For the description of the apparatus we may refer to the earlier paper¹⁾. There are some slight modifications: in order to detect neutral particles a second multiplier was included. This was done to investi-

gate the inelastic collisions $K^+ + B \rightarrow K + B^+$ and $Cl^- + B \rightarrow Cl + [B + e]$, where B denotes the noble gas atom. As the Cl^- ions are produced by evaporating KCl from a hot tungsten wire we could instead of a K^+ beam easily get a Cl^- beam by inverting the electric and magnetic fields in the apparatus. The intensity of the Cl^- ion beam is about a hundred times lower than the intensity of the K^+ ion beam, which gives an ion current of 10^{-9} A at higher energies. While the $K^+ - B$ collision cross sections have been measured in the energy range from 150 through 4000 eV, the $Cl^- - B$ measurements have been made in the energy range from 2400 through 4000 eV. The reduction of the energy range of the latter is a consequence of the negative voltage of the first dynode of the multiplier, which slows down the negative ions. This results in a considerable decrease of sensitivity and, as a consequence, in a smaller energy range. The large number of electrons in the source gives rise to a considerable space charge which suppresses the Cl^- emission. To get rid of this effect we applied a small electric field in the source, which gave an important increase in intensity.

3. *Results.* The total incomplete cross section for elastic scattering, σ is given by:

$$\sigma = \frac{1}{nl} \cdot \ln \frac{I_0}{I_p},$$

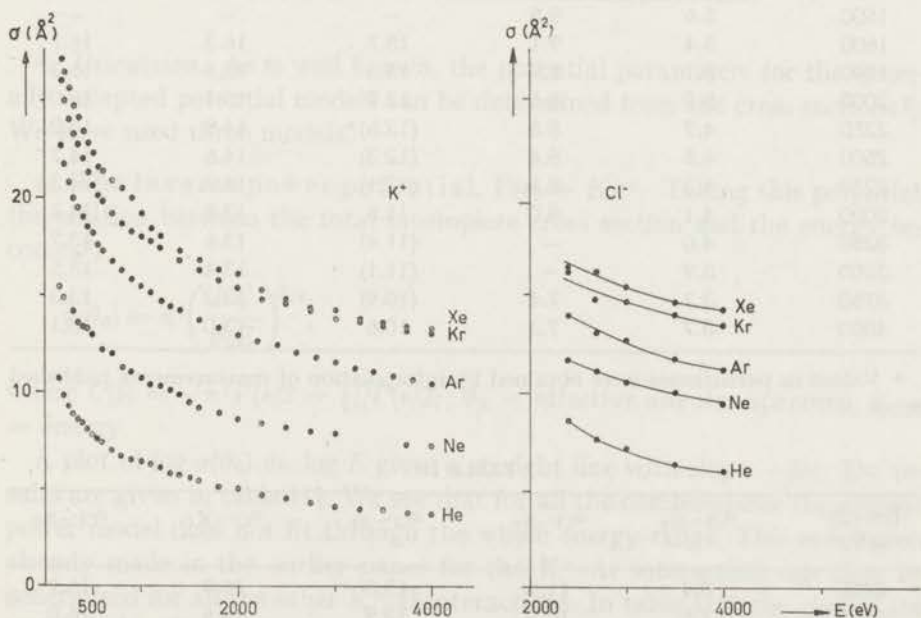


Fig. 1. Incomplete total cross sections for the interaction of K^+ and Cl^- ions with noble gas atoms.

TABLE I

Total incomplete cross sections for elastic scattering (in Å²) of K⁺ and Cl⁻ ions
vs. noble gas atoms in the energy range from 150 through 4000 eV

TABLE IA

Energy (eV)	σ_{K^+-He}	σ_{K^+-Ne}	σ_{K^+-Ar}	σ_{K^+-Kr}	σ_{K^+-Xe}
150	10.7	15.6	23.0	26.0	27.0
200	9.8	15.1	22.0	25.0	26.3
250	9.3	14.6	21.1	24.0	25.5
300	8.9	14.3	20.3	23.3	24.6
350	8.6	13.8	19.7	22.8	23.9
400	8.4	13.6	19.2	22.0	23.3
450	8.1	13.4	18.7	21.3	22.7
500	7.8	13.2	18.2	20.7	22.2
550	7.6	—	17.8	20.2	21.5
600	7.4	11.9	17.4	19.8	21.3
700	7.0	11.7	16.8	19.2	20.2
800	6.7	11.4	16.3	18.7	20.4
900	6.5	11.0	15.8	18.3	19.9
1000	6.4	10.7	15.4	18.0	19.1
1100	6.3	10.2	15.1	17.8	18.3
1200	6.1	10.0	14.7	17.5	18.0
1300	5.8	9.9	14.4	—	—
1400	5.7	9.2	14.2	16.8	17.2
1500	5.6	9.5	—	—	—
1600	5.4	9.1	13.7	16.3	16.7
1800	5.1	8.9	13.3	15.8	16.2
2000	5.0	8.6	12.9	15.4	16.0
2250	4.7	8.5	(12.6) ^a	14.8	15.2
2500	4.5	8.4	(12.3)	14.6	14.7
2750	4.3	8.2	(12.1)	14.2	14.3
3000	4.1	8.0	11.6	13.8	14.2
3250	4.0	—	(11.4)	13.6	13.7
3500	3.9	—	(11.1)	13.4	13.5
3750	3.7	7.4	(10.9)	13.2	13.3
4000	3.7	7.3	10.6	13.0	13.1

^a Values in parentheses were obtained by interpolation of measurements published in ref. 1.

TABLE IB

Energy (eV)	σ_{Cl^-He}	σ_{Cl^-Ne}	σ_{Cl^-Ar}	σ_{Cl^-Kr}	σ_{Cl^-Xe}
2400	8.4	11.5	13.8	16.0	16.1
2700	7.5	10.9	12.9	14.6	16.0
3000	6.9	10.4	12.6	14.5	15.3
3500	6.2	9.9	11.6	13.8	14.5
4000	5.8	9.3	11.0	13.3	14.1

where n is the number of target particles per unit volume; $I_{0,p}$ is the beam intensity without and with attenuation; l is the effective scattering length.

In table Ia and Ib the results of our K⁺- respectively Cl⁻ vs. noble gas cross section measurements are given as a function of the energy of the primary beam (fig. 1).

The accuracy of the relative measurements is better than 1%. The absolute values of the cross sections, however, have an accuracy of 4% for the K⁺ ion measurements and 10% for the Cl⁻ measurements.

Finally we measured the cross sections for the inelastic process K⁺ + B → K + B⁺. We used a second detector with which we could measure the intensity of neutral K atoms coming from this process. The results of two combinations are given in table II.

TABLE II

Total incomplete cross sections (in Å ²) for the charge exchange process K ⁺ + B → K + B ⁺ in the energy range from 1000 through 4000 eV		
$E(\text{eV})$	$\sigma_{\text{exch}}(\text{K}^+-\text{Ar})$	$\sigma_{\text{exch}}(\text{K}^+-\text{Xe})$
1000	0.5×10^{-4}	0.8×10^{-4}
2000	0.6×10^{-4}	1.5×10^{-4}
3000	1.0×10^{-4}	2.5×10^{-4}
4000	2.6×10^{-4}	9.0×10^{-4}

4. *Discussion.* As is well known, the potential parameters for the generally accepted potential models can be determined from the cross sections²⁾. We have used three models.

a) The inverse power potential, $V(r) = K/r^s$. Taking this potential, the relation between the total incomplete cross section and the energy becomes²⁾

$$\sigma(\vartheta_0) = \pi \cdot \left(\frac{KC}{\vartheta_0 E} \right)^{2/s},$$

where $C(s) = \sqrt{\pi} \cdot \Gamma(s/2 + \frac{1}{2}) / \Gamma(s/2)$; ϑ_0 = effective angular aperture; E = energy.

A plot of $\log \sigma(\vartheta_0)$ vs. $\log E$ gives a straight line with slope $-2/s$. The results are given in table III. We see that for all the combinations the inverse power model does not fit through the whole energy range. This conclusion already made in the earlier paper for the K⁺-Ar interaction can thus be generalized for all the other K⁺-B interactions. In table IIIb the results are given of the Cl⁻-B interaction. As the energy range was relatively small, we could do with only one single set of parameters.

TABLE III

Potential parameters for the interaction between K^+ , Cl^- and noble gas atoms for the inverse power model, $V(r) = K/r^s$

TABLE IIIA				
Combination	$K(eV \cdot \text{\AA}^s)$		s	range (\AA)
K^+-He	5.9	± 0.7	4.71 ± 0.28	1.09-1.28
	10.8	± 1.2	7.09 ± 0.22	1.28-1.86
K^+-Ne	48	± 11	5.93 ± 0.59	1.48-1.93
	240	± 45	8.40 ± 0.42	1.93-2.07
K^+-Ar	135	± 16	6.01 ± 0.12	1.85-1.98
	540	± 60	8.30 ± 0.08	1.98-2.46
	2940	± 430	10.27 ± 0.31	2.46-2.66
K^+-Kr	610	± 70	8.06 ± 0.24	2.03-2.13
	1600	± 290	9.35 ± 0.37	2.13-2.88
K^+-Xe	6600	± 1500	7.41 ± 0.37	2.04-2.42
	13400	± 3500	10.81 ± 0.54	2.42-2.95

TABLE IIIB

Combination	$K(eV \cdot \text{\AA}^s)$		s	range (\AA)
Cl^-He	12.9	± 1.7	2.74 ± 0.16	1.37-1.65
Cl^-Ne	51.6	± 5.7	4.65 ± 0.09	1.70-1.93
Cl^-Ar	95	± 17	5.00 ± 0.35	1.89-2.11
Cl^-Kr	285	± 45	6.06 ± 0.24	2.07-2.27
Cl^-Xe	280	± 40	5.88 ± 0.18	2.13-2.32

The error in the s -parameter is determined graphically, as well as the error in α and a in tables IV and V. The main contribution in the error in K (respectively A and C) comes from the error in s (respectively α and a).

b) The exponential model $V(r) = A e^{-\alpha r}$. For this potential the cross section is given by³⁾

$$[\sigma(\vartheta_0)]^{\frac{1}{2}} = \frac{\pi^{\frac{1}{2}}}{\alpha} \cdot \ln \left\{ \pi^{\frac{1}{2}} \left(\frac{\alpha}{2} \right)^{\frac{1}{2}} \cdot \frac{A}{\vartheta_0} \right\} + \frac{\pi^{\frac{1}{2}}}{\alpha} \cdot \ln \{ [\sigma(\vartheta_0)]^{\frac{1}{2}} / E \},$$

so that a plot of $[\sigma(\vartheta_0)]^{\frac{1}{2}}$ vs. $\ln \{ [\sigma(\vartheta_0)]^{\frac{1}{2}} / E \}$ should give a straight line with slope $\pi^{\frac{1}{2}}/\alpha$. The results are given in table IVa, b (fig. 2). For each combination we could do with one single set of parameters so that we may conclude that this potential model gives a satisfactory representation of the interaction over a large internuclear range ($\sim 1 \text{ \AA}$). This is an experimental affirmation of what theoretically also is found^{4,5)}. The potentials according to the potential parameters in table IV are plotted in fig. 3.

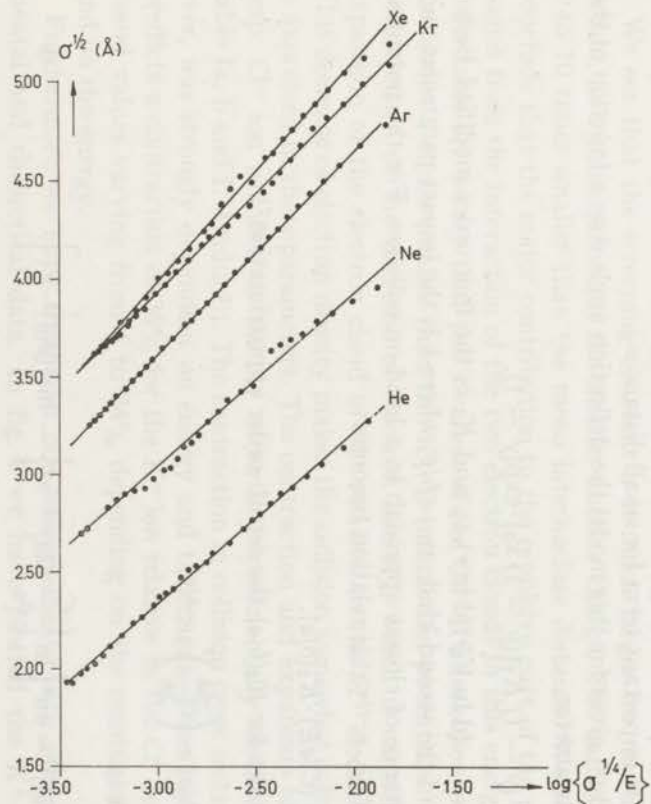


Fig. 2. Incomplete total cross sections are plotted as to obtain the potential parameters for the exponential model, for the combinations K^+-B .

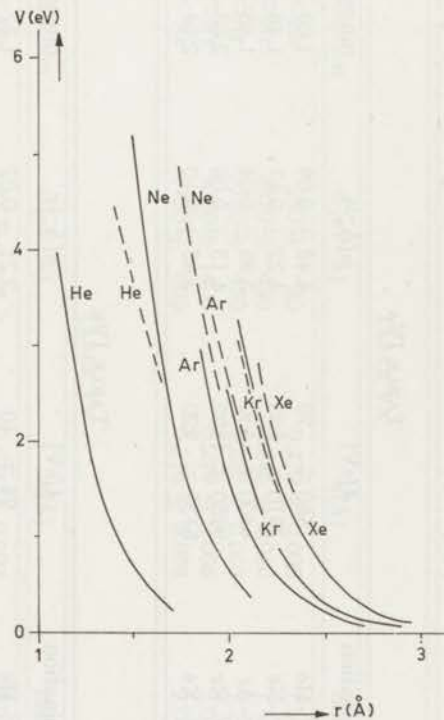


Fig. 3. Interaction energy as a function of the internuclear osepuration for the combinatins K^+-B (drawn curves) and the combinations $Cl^- - B$ (dashed curves).

TABLE IV

Potential parameters for the interaction between K^+ , Cl^- and noble gas atoms for the exponential model $V(r) = A \cdot e^{-\alpha r}$

Combination	A (eV)	α (\AA^{-1})	range (\AA)
K^+ -He	550 \mp 70	4.48 \pm 0.09	1.09-1.86
K^+ -Ne	2910 \mp 580	4.22 \pm 0.17	1.48-2.07
K^+ -Ar	4400 \mp 530	3.95 \pm 0.04	1.85-2.66
K^+ -Kr	9950 \mp 1500	4.13 \pm 0.08	2.03-2.88
K^+ -Xe	5130 \mp 920	3.63 \pm 0.10	2.04-2.95

Combination	A (eV)	α (\AA^{-1})	range (\AA)
Cl^- -He	94 \mp 10	2.21 \pm 0.02	1.37-1.65
Cl^- -Ne	660 \mp 70	3.02 \pm 0.03	1.70-1.93
Cl^- -Ar	480 \mp 60	2.59 \pm 0.05	1.89-2.11
Cl^- -Kr	2060 \mp 330	3.14 \pm 0.09	2.07-2.27
Cl^- -Xe	3550 \mp 650	3.33 \pm 0.10	2.13-2.32

c) The screened Coulomb potential $V(r) = (C/r) e^{-r/a}$. This model is physically more meaningful than the two other models. (For $r \ll a$ this potential has a $1/r$ behaviour, which represents the nuclear repulsion, which is the most important term for small distances.)

Baroody⁶) gives for this model the deflection angle ϑ as a function of the impact parameter,

$$\vartheta = (\gamma - 1) K_1\{(\gamma - 1) x_0\} \cdot \exp(\gamma - 1),$$

where $\gamma = -\{d \ln V(r)/d \ln r\}_{r=p}$ and K_1 is the first order modified Bessel function of the second kind; $x_0 = b/p$, where b is the impact parameter and p the distance of closest approach in a head-on collision. For the potential $V(r) = (C/r) \cdot e^{-r/a}$ this relation becomes

$$\vartheta = (C/aE) \cdot K_1(b/a).$$

If we take for $K_1(b/a)$ the zeroth-order approximation⁷)

$$K_1(b/a) \simeq \left(\frac{\pi a}{2b}\right)^{\frac{1}{2}} \cdot e^{-b/a},$$

the result is

$$[\sigma(\vartheta_0)]^{\frac{1}{2}} = a\pi^{\frac{1}{2}} \left[\ln \left\{ \frac{C}{\vartheta_0} (2a)^{-\frac{1}{2}} \cdot \pi^{\frac{1}{2}} \right\} - \ln \{[(\vartheta_0)]^{\frac{1}{2}} \cdot E\} \right].$$

TABLE V

Potential parameters for the interaction between K⁺, Cl⁻ and noble gas atoms for the screened Coulomb model $V(r) = (C/r) e^{-r/a}$

TABLE VA

Combination	$C(\text{eV} \cdot \text{\AA})$	$a(\text{\AA})$	range (\AA)
K ⁺ -He	250 ± 30	0.272 ± 0.005	1.09-1.86
K ⁺ -Ne	2520 ± 450	0.245 ± 0.010	1.48-2.07
K ⁺ -Ar	3750 ± 450	0.287 ± 0.003	1.25-2.66
K ⁺ -Kr	9000 ± 1400	0.279 ± 0.005	2.03-2.88
K ⁺ -Xe	4450 ± 800	0.314 ± 0.009	2.04-2.95

TABLE VB

Combination	$C(\text{eV} \cdot \text{\AA})$	$a(\text{\AA})$	range (\AA)
Cl ⁻ -He	57.7 ± 6.3	0.674 ± 0.007	1.37-1.65
Cl ⁻ -Ne	470 ± 50	0.411 ± 0.004	1.70-1.93
Cl ⁻ -Ar	340 ± 40	0.496 ± 0.010	1.89-2.11
Cl ⁻ -Kr	1620 ± 260	0.380 ± 0.011	2.07-2.27
Cl ⁻ -Xe	2270 ± 390	0.368 ± 0.012	2.13-2.32

Also for this model we could find one single set of parameters. Table Va, b gives again the parameters together with the range of validity.

We see that the screening constant a is much larger for the Cl⁻ interaction, as a consequence of the smaller nuclear charge. The values of a are 2 to 10 times smaller than the mean internuclear distance. We thus may conclude that the major contribution to the repulsive part of the potential comes from the interaction of the two electron clouds in this energy range.

In table III we see that the s values of the Cl⁻-B interaction potentials are about 2 times smaller than the K⁺-B interaction potentials. This is a consequence of the decrease of electron density, which is caused by the expansion of the electron cloud of Cl⁻ relative to the K⁺ electron cloud. This decrease of electron density makes the collision somewhat softer which is expressed in the s -parameters. The contraction and expansion of the K⁺ resp. Cl⁻ ion relative to the Ar atom is experimentally confirmed (see table Ia, b and I. Amdur⁸). The contraction in collision cross section, however, was strongly dependent on energy and target gas. Theoretically one predicts a contraction of 36% for the K⁺ ion relative to the Cl⁻ ion⁹). We found values varying from 6 to 24% depending on the combination used and on the energy.

Furthermore we have compared our measurements with other experimental and theoretical data. In fig. 4 we have plotted the K⁺-Ar and

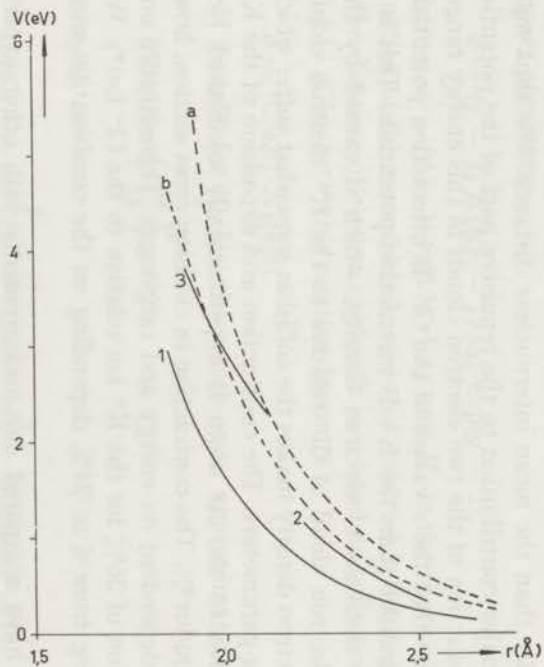


Fig. 4. Interaction potentials.

- calculated a. Ar-Ar potential (A. A. Abrahamson¹⁰)
 b. K⁺-Ar potential (D. W. Sida¹¹)
 ——— measured 1. K⁺-Ar potential (this work)
 2. Ar-Ar potential (I. Amdur⁸)
 3. Cl⁻-Ar potential (this work)

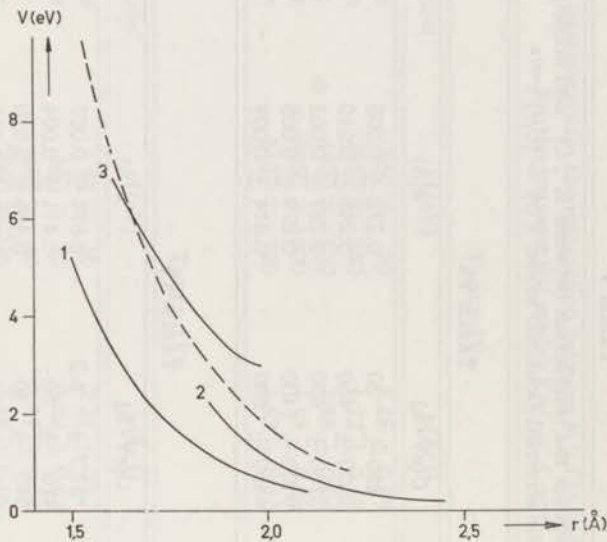


Fig. 5. Interaction potentials.

- calculated Ar-Ne potential (R. K. Nesbet⁵)
 1. K⁺-Ne potential (this work)
 ——— measured 2. Ar-Ne potential (I. Amdur¹⁰)
 3. Cl⁻-Ne potential (this work)

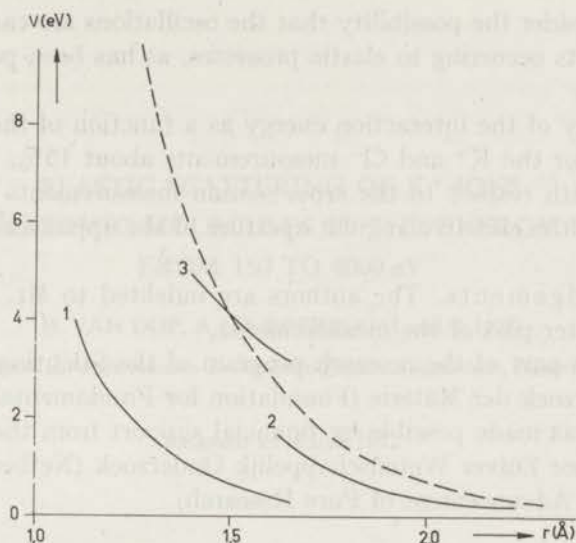


Fig. 6. Interaction potentials.

- - - - calculated Ar-He potential (R. K. Nesbet⁵)
 ——— measured 1. K^+ -He potential (this work)
 2. Ar-He potential (I. Amdur¹⁵)
 3. Cl^- -He potential (this work)

Cl^- -Ar potential according to table IV, together with the Ar-Ar potential as measured by Amdur⁸) and calculated by A. A. Abrahamson¹⁰), and also the K^+ -Ar potential as calculated by D. W. Sida¹¹). There is a good agreement with the Amdur experiment but a certain discrepancy between theory and experiment. In figs. 5 and 6 we have plotted some potentials for the Ne and He case. We found in general the same structure as in fig. 4 and we can make the same remarks as about the Ar case.

Plotting the total cross sections against energy we observed for all combinations small oscillations (fig. 2). As our relative accuracy was lying within the amplitude of these oscillations we searched for an explanation of these oscillations. First we investigated whether inelastic effects caused the oscillations. The inelastic processes $K^+ + B \rightarrow K + B^+$ or $Cl^- + B \rightarrow Cl + B + e$ were experimentally cancelled. In table II we see that the cross sections are below 10^{-3} \AA^2 . These values are too small to explain the observed oscillations.

Excitation effects seem very unlikely. An experiment done by Forst¹²) who selected the resulting ions from the process $Li^+ + B \rightarrow Li^+ + B^*$ on energy, showed that no energy losses greater than 4 eV occurred which is far less than the first excited level of any of the noble gases.

Another possible explanation has been indicated by Schoenebeck¹³), who introduces a screened induction potential of the form $1/(r^4 + a^4)$.

We also consider the possibility that the oscillations are caused by small quantum effects occurring in elastic processes, as has been pointed out by Smith *et al.*¹⁴).

The accuracy of the interaction energy as a function of the internuclear separation is for the K^+ and Cl^- measurements about 15%. This decrease in accuracy with respect to the cross section measurements is due to the uncertainty of the effective angular aperture of the apparatus.

Acknowledgements. The authors are indebted to Mr. G. Kleyn for doing the greater part of the measurements.

This work is part of the research program of the Stichting voor Fundamenteel Onderzoek der Materie (Foundation for Fundamental Research on Matter) and was made possible by financial support from the Nederlandse Organisatie voor Zuiver Wetenschappelijk Onderzoek (Netherlands Organization for the Advancement of Pure Research).

REFERENCES

- 1) Amdur, I., Inouye, H., Boerboom, A. J. H., v. d. Steege, A. N., Los, J. and Kistemaker, J., *Physica* **41** (1969) 566.
- 2) See for instance Kennard, E. H., *Kinetic Theory of Gases* (New York, London, 1932) 115.
- 3) Bernstein, R. B., *J. chem. Phys.* **38** (1963) 515.
- 4) Abrahamson, A. A., *Phys. Rev.* **178** (1969) 76.
- 5) Nesbet, R. K., *J. chem. Phys.* **48** (1968) 1419.
- 6) Baroody, E. M., *Phys. of Fluids* **5** (1962) 925.
- 7) MacRobert, T. M., *Spherical Harmonics* (Oxford, London, Edinburgh, Toronto, Sydney, Paris, Braunschweig, 1967).
- 8) Amdur, I. and Mason, E. A., *J. chem. Phys.* **22** (1954) 670.
- 9) Gombàs, P., *Handbuch der Physik*, vol. XXXVI (Berlin, Göttingen, Heidelberg, 1950).
- 10) Abrahamson, A. A., *Phys. Rev.* **130** (1963) 693.
- 11) Sida, D. W., *Thesis*, London (1956).
- 12) Forst, G., *Z. angew. Phys.* **20** (1966) 265.
- 13) Schoenebeck, H., *Z. Phys.* **177** (1964) 8.
- 14) Smith, F. J., Mason, E. A. and Vanderslice, J. T., *J. chem. Phys.* **42** (1965) 3257.
- 15) Amdur, I., Mason, E. A. and Harkness, A. L., *J. chem. Phys.* **22** (1954) 1071.
- 16) Amdur, I. and Mason, E. A., *J. chem. Phys.* **25** (1956) 632.

ELASTIC SCATTERING OF K^+ IONS
FROM DIATOMIC MOLECULES IN THE ENERGY RANGE
FROM 150 TO 4000 eV

H. VAN DOP, A.J.H. BOERBOOM and J. LOS

FOM-Instituut voor Atoom- en Molecuulfysica, Amsterdam, Nederland

Received 13 March 1972

Synopsis

Potential parameters are determined for the combinations K^+ - H_2 , HD, D_2 , N_2 , $C^{16}O$ and $C^{18}O$. The best description for the interaction is given by an exponential potential. The (small) differences in cross section between the iso-electronic molecules are within the experimental error. A correlation, however, is observed between the asymmetry of the molecules and the measured cross sections.

In addition to measurements of potential parameters for ion-atom scattering¹⁾ some ion-molecule potentials are determined. Cross sections have been evaluated for elastic scattering of K^+ ions from H_2 , D_2 , HD, N_2 and CO. In the original setup of this experiment it was our aim to compare the cross sections of the isotopic molecules H_2 , HD and D_2 and of the iso-electronic molecules N_2 and CO. (Apart from the normal CO also the isotopic $C^{18}O$ was used.) In some calculations, namely, small differences in the cross sections of isotopic molecules are predicted. Fowler *et al.*²⁾, who did similar experiments, using a helium beam, ascribed these differences to a contribution of rotational excitation and de-excitation³⁾. In our opinion, based on a calculation tentatively done by one of the authors, the difference in cross section can be explained by the displacement of the centre of mass relative to the charge distribution, the latter being the same for isotopic molecules. The calculations show that when the displacement is a the contribution to the cross section is approximately $\frac{3}{2}\pi a^2$. This means an increase in the cross section of HD of about 0.5%.

The measurements were performed in the apparatus described in an earlier paper⁴⁾. The inverse power potential $V(r) = K/r^5$, the exponential potential $V(r) = Ae^{-\alpha r}$ and the screened Coulomb potentials $V(r) = (C/r)e^{-r/a}$ have been

* A previously determined value of the angular aperture of the apparatus (2.60×10^{-3} radians) has been proven to be too low. As a consequence the values of the potentials in ref. 1 are about 70% too small.

TABLE I

Potential parameters of the inverse power potential model $V(r) = K/r^s$ †

Combination	K (eV Å ^s)	s	Range (Å)
K ⁺ -H ₂	241	8.67 ± 0.64	2.31-2.09
	79.3	7.00 ± 0.16	2.09-1.79
	25.8	4.67 ± 0.12	1.79-1.33
K ⁺ -HD	349	8.73 ± 0.11	2.38-2.16
	70.7	6.47 ± 0.16	2.16-1.83
	29.5	4.74 ± 0.23	1.83-1.36
K ⁺ -D ₂	304	8.61 ± 0.37	2.36-2.14
	66.8	6.45 ± 0.10	2.14-1.82
	24.3	4.33 ± 0.18	1.82-1.32
K ⁺ -N ₂	5309	10.11 ± 0.25	2.79-2.37
	147	5.55 ± 0.25	2.37-1.76
K ⁺ -C ¹⁶ O	17670	11.50 ± 0.61	2.75-2.38
	192	5.87 ± 0.15	2.38-1.79
K ⁺ -C ¹⁸ O	36408	12.03 ± 0.94	2.79-2.41
	139	5.35 ± 0.27	2.41-1.77

† An error in K is not given as it is strongly correlated to the error in s . The uncertainty in the potential is estimated to be 20%.

TABLE II

Potential parameters of the exponential potential model $V(r) = Ae^{-\alpha r}$ ‡

Combination	A (eV)	α (Å ⁻¹)	Range (Å)
K ⁺ -H ₂	893	3.68 ± 0.06	2.31-1.33
K ⁺ -HD	751	3.47 ± 0.04	2.38-1.36
K ⁺ -D ₂	635	3.40 ± 0.05	2.36-1.32
K ⁺ -N ₂	2619	3.43 ± 0.07	2.79-2.37
	1208	3.01 ± 0.05	2.37-1.76
K ⁺ -C ¹⁶ O	4413	3.66 ± 0.09	2.75-2.38
	1635	3.13 ± 0.07	2.38-1.79
K ⁺ -C ¹⁸ O	2647	3.38 ± 0.11	2.79-2.41
	1009	2.87 ± 0.06	2.41-1.77

‡ See footnote table I.

TABLE III

Potential parameters of the screened Coulomb model $V(r) = (C/r) e^{-r/a}$

Combination	C (eV Å)	a (Å)	Range (Å)
K^+-H_2	635	0.320 ± 0.007	2.31-1.33
K^+-HD	549	0.342 ± 0.005	2.38-1.36
K^+-D_2	461	0.350 ± 0.007	2.36-1.32
K^+-N_2	2313	0.335 ± 0.009	2.79-2.37
$K^+-C^{16}O$	976	0.399 ± 0.010	2.37-1.76
	3911	0.310 ± 0.009	2.75-2.38
$K^+-C^{18}O$	1331	0.379 ± 0.012	2.38-1.79
	2384	0.339 ± 0.11	2.79-2.41
	828	0.420 ± 0.13	2.41-1.77

* See footnote table I.

fitted to the experimental data. The results are given in tables I, II and III. They fitted best to an exponential potential over the investigated range of ion-molecule separation. For the molecules N_2 and CO it was not possible to fit the experimental data to one single set of parameters of the exponential potential.

The cross sections unfortunately all coincide within the experimental error, which is about 4%. A general conclusion, however, is that the cross sections tend to be somewhat higher for the asymmetric molecules HD and $C^{18}O$. The same

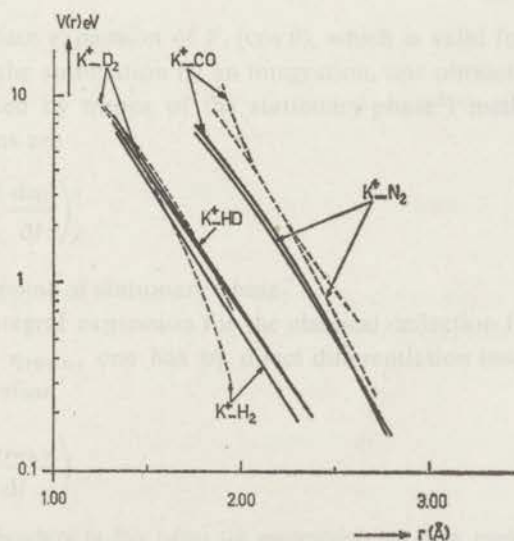


Fig. 1. Interaction potentials: --- measurements of ref. 5; — this work.

tendency is expressed in the potentials as is shown in fig. 1. It is striking that this conclusion is established by Fung *et al.*⁵⁾ for N_2 and CO. They also measured a somewhat lower cross section – and consequently a lower potential – for H_2 than for D_2 (*cf.* fig. 1), though they should be essentially the same.

The measurements of Fung *et al.*⁵⁾ show a steeper descent of the K^+-H_2 and K^+-D_2 potential at large ion-molecule separation. The N_2 and CO potentials are somewhat shifted compared with ref. 5, but they have about the same slope.

Acknowledgement. This work is sponsored by F.O.M. with financial support by Z.W.O.

REFERENCES

- 1) Boerboom, A.J.H., Van Dop, H. and Los, J., *Physica* **46** (1970) 458.
- 2) Fowler, M.C., Jordan, J.E. and Amdur, I., VI ICPEAC, Book of Abstracts, p. 516, M.I.T. Press (Cambridge (Mass.), 1969).
- 3) Cross, R.J. and Gordon, R.G., *J. chem. Phys.* **45** (1966) 3571.
- 4) Amdur, I., Inouye, H., Boerboom, A.J.H., Van der Steege, A.N., Los, J. and Kistemaker, J., *Physica* **41** (1969) 566.
- 5) Fung, L. W-M, Ph. D. Thesis, M.I.T. 1971; Hance, R.L., Ph. D. Thesis, M.I.T. 1970; Johnson, S.E., Ph. D. Thesis, M.I.T. 1971.

THE SEMICLASSICAL EQUIVALENCE IN THE CASE OF NONSPHERICAL SCATTERING

H. VAN DOP and A. TIP

FOM-Instituut voor Atoom- en Molecuulfysica, Amsterdam, Nederland

Received 17 January 1972

Synopsis

The stationary-phase method is applied to the eikonal amplitude for elastic small-angle scattering, both in the case of spherical, and nonspherical scattering. The correspondence between the resulting equations and the classical scattering formulae is shown, and some semiclassical equivalence relations are derived.

1. *Introduction.* The semiclassical equivalence for scattering from symmetric potentials is well known. Following the partial-wave method¹⁾, the scattering amplitude $f(\theta)$, is expressed in terms of the phase shifts $\eta_l(k)$,

$$f(\theta) = \frac{1}{2ik} \sum_{l=0}^{\infty} (2l+1) \exp [2i\eta_l(k)] P_l(\cos \theta), \quad (\theta \neq 0, \pi). \quad (1)$$

Using the Laplace expansion of $P_l(\cos \theta)$, which is valid for large l and $l\theta \gg 1$, and replacing the summation by an integration, one obtains an expression which can be evaluated by means of the stationary-phase²⁾ method. The stationary-phase conditions are

$$\frac{1}{2}\theta_e = \pm \left(\frac{d\eta_l}{dl} \right)_e \quad (2)$$

where l is the point of stationary phase[†].

From the integral expression for the classical deflection function $\Theta(b)$ and the JWKB phase, η_{JWKB} , one has by direct differentiation (and using $l = kb$) the well-known relation

$$\frac{1}{2}\Theta = \left(\frac{d\eta_{\text{JWKB}}}{dl} \right)_e, \quad (3)$$

[†] Here and elsewhere in this paper the assumption has been made, that there is only one point of stationary phase (l).

which in view of eq. (2) is known as the semiclassical equivalence relationship³). The evaluation of the integral over l yields

$$f(\theta) = \left[\frac{b'}{\sin \theta} \left| \frac{db'}{d\theta} \right| \right]^{\frac{1}{2}} e^{i\gamma}, \quad (4)$$

where γ is a phase factor. After squaring, this results in the classical expression for the differential cross section.

In this paper the procedure, which is briefly outlined above will be followed in the case of scattering by a nonspherical potential. The starting point, however, will be the eikonal scattering amplitude, as the Schrödinger equation is not separable for a nonspherical potential, so that the partial-wave analysis becomes more cumbersome than in the spherically symmetric case.

2. *The eikonal approximation.* The eikonal approximation⁴) gives an analytic expression for the scattering amplitude using an arbitrary potential. The only validity condition for this approximation seems to be $ka \gg 1^5$), where k is the wavenumber of the scattered particle and a is a measure of the range of the potential (it is assumed that the potential drops sufficiently fast to zero for large distances). When the centre of the potential is chosen in the origin of a coordinate frame, having its Z axis parallel to the initial direction of the momentum k_i , and when k_f is the final momentum, the eikonal amplitude for elastic scattering is given by

$$f(k_i, k_f) = -\frac{m}{2\pi\hbar^2} \int d^3r \exp [i(k_i - k_f) \cdot r] V(r) \exp \left[-\frac{i}{\hbar v} \int_{-\infty}^z V(r) dz' \right], \quad (5)$$

where $|k_i| = |k_f| = k$, and v is the velocity of the incident particle (cf. fig. 1). For small-angle scattering this expression reduces to⁶

$$f(k_i, k_f) = \frac{k}{2\pi i} \int d^2b \exp [i(k_i - k_f) \cdot b] \left\{ \exp \left[-\frac{i}{\hbar v} \int_{-\infty}^{+\infty} V(r) dz' \right] - 1 \right\}, \quad (6)$$

where b is a vector in the X - Y plane having magnitude b' and azimuthal angle ψ . The limitation of the scattering angle θ is given by

$$\theta \lesssim 1/(ka)^{\frac{1}{2}}. \quad (7)$$

Expression (6) will be used for a semiclassical treatment.

* If the Z axis is chosen perpendicular to the momentum transfer $k_i - k_f$, then eq. (6) is valid for all angles⁵) (provided $ka \ll 1$).

In that case, however, the classical interpretation of b' as an impact parameter fails at large angles.

2.1. Spherically symmetric potential. By expressing the Legendre polynomials in (1) by an asymptotic relation for small angles and large l , Glauber and Franco^{4,8} established the correspondence between the partial-wave expansion for the scattering amplitude and (6), both in the case of spherical and nonspherical potentials.

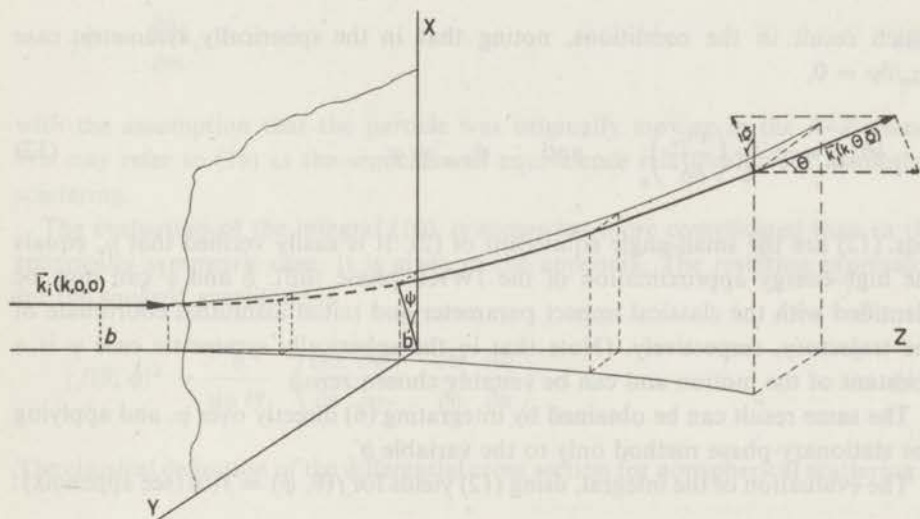


Fig. 1. The geometry of the collision.

So it should not be surprising that if (6) is submitted to the stationary-phase method, results, similar to those described in the introduction, are obtained. Indeed, we have, using the notations

$$\eta_e(b', \psi) = \frac{1}{2\hbar v} \int_{-\infty}^{+\infty} V(b' + nz) dz, \quad (8)$$

where n is a unit vector in the Z direction and v the initial velocity of the particle, and

$$g(b', \psi) = -(k_i - k_f) \cdot b' + 2\eta_e(b', \psi), \quad (9)$$

the integral

$$f(\theta, \phi) = \frac{k}{2\pi i} \int_0^{\infty} db' \int_0^{2\pi} d\psi b' \exp[-ig(b', \psi)], \quad (10)$$

with $\theta, \phi \neq 0$. The main contribution to the integral will come from the region(s) where the function $g(b', \psi)$ has a stationary point of order one or higher, the former only being considered:

$$\left(\frac{\partial g}{\partial b'}\right)_b = 0 \quad \text{and} \quad \left(\frac{\partial g}{\partial \psi}\right)_\psi = 0, \quad (11)$$

which result in the conditions, noting that in the spherically symmetric case $\partial \eta_e / \partial \psi = 0$,

$$\frac{1}{2}\theta_{b,\varphi} = \pm \frac{1}{k} \left(\frac{\partial \eta_e}{\partial b'}\right)_b \quad \text{and} \quad \phi_{b,\varphi} = \varphi. \quad (12)$$

Eqs. (12) are the small-angle equivalent of (2). It is easily verified that η_e equals the high-energy approximation of the JWKB phase shift. b and φ can now be identified with the classical impact parameter and initial azimuthal coordinate of the trajectory, respectively. (Note that in the spherically symmetric case φ is a constant of the motion and can be suitably chosen zero.)

The same result can be obtained by integrating (6) directly over ψ , and applying the stationary-phase method only to the variable b' .

The evaluation of the integral, using (12) yields for $f(\theta, \phi) = f(\theta)$ (see appendix):

$$|f(\theta)|^2 = \frac{b}{\sin \theta} \left| \frac{\partial b}{\partial \theta} \right|. \quad (13)$$

We may conclude that in the stationary-phase approximation the eikonal amplitude, in its range of validity, has the same classical correspondence as the partial-wave series expansion in the case of spherical scattering.

2.2. Nonspherical potential. Again we apply the stationary phase approximation to the eikonal amplitude. It leads to the equations (see appendix)

$$\sin \theta_{b,\varphi} = \frac{1}{k} \left\{ \left(\frac{\partial \eta_e}{\partial b'}\right)_{b,\varphi}^2 + \frac{1}{b'^2} \left(\frac{\partial \eta_e}{\partial b'}\right)_{b,\varphi}^2 \right\}^{\frac{1}{2}}, \quad (14a)$$

$$\text{tg}(\varphi - \phi_{b,\varphi}) = -\frac{1}{b'} \left(\frac{\partial \eta_e}{\partial \psi}\right)_{b,\varphi} \left\{ \left(\frac{\partial \eta_e}{\partial b'}\right)_{b,\varphi} \right\}^{-1}. \quad (14b)$$

When (14a) and (14b) are compared with the classical expressions for the deflection angles θ and ϕ in the case of small-angle scattering from a nonspherical potential⁶, one is justified in considering b and φ as the classical impact parameter and the initial azimuthal position of the scattered particle, respectively.

Eq. (14b) can be written in a more compact form by introducing the z component of the angular momentum of the particle during the scattering,

$$l_z \equiv m = -kb \sin \theta \sin (\varphi - \phi). \quad (15)$$

(14) and (15) can then be combined to give

$$\frac{1}{2}\Phi = \frac{\partial \eta_e}{\partial m}, \quad (16)$$

with the assumption that the particle was originally moving in the X - Z plane. We may refer to (16) as the semiclassical equivalence relationship for azimuthal scattering.

The evaluation of the integral (10), is somewhat more complicated than in the spherically symmetric case. It is given in the appendix. The resulting expression for the squared amplitude is

$$|f(\theta, \phi)|^2 = \frac{b}{\sin \theta} \cdot \left(\frac{\partial \theta}{\partial b} \frac{\partial \Phi}{\partial \varphi} - \frac{\partial \theta}{\partial \varphi} \frac{\partial \Phi}{\partial b} \right)^{-1}. \quad (17)$$

The classical definition of the differential cross section for nonspherical scattering is

$$\frac{d\sigma}{d\Omega} \sin \theta \, d\theta \, d\Phi = b \, db \, d\varphi. \quad (18)$$

Considering b and φ as the independent variables, $d\theta \, d\Phi$ can be expressed in terms of $db \, d\varphi$:

$$d\theta \, d\Phi = J(\theta, \Phi; b, \varphi) \, db \, d\varphi, \quad (19)$$

where

$$J(\theta, \Phi; b, \varphi) = \frac{\partial \theta}{\partial b} \frac{\partial \Phi}{\partial \varphi} - \frac{\partial \theta}{\partial \varphi} \frac{\partial \Phi}{\partial b}.$$

When (19) is substituted in (18), we see that (17) is the classical definition of the differential cross section for scattering from a nonspherical potential.

Acknowledgement. The authors would like to thank Dr. D.J. Auerbach for his comments on the manuscript. Their thanks also go to Professor C.J. Joachain for fruitful discussion and for critically reading the manuscript.

This work is part of the research program of the Stichting voor Fundamenteel Onderzoek der Materie (Foundations for Fundamental Research on Matter) and

was made possible by financial support from the Nederlandse Organisatie voor Zuiver-Wetenschappelijk Onderzoek (Netherlands Organization for the Advancement of Pure Research).

APPENDIX

The evaluation of the integral

$$f(\theta, \phi) = \frac{k}{2\pi i} \int_0^{\infty} db' \int_0^{2\pi} d\psi b' \exp[-ig(b', \psi)].$$

I. *Spherically symmetric case.* In this case the phase shift η_e depends only on b' , so that

$$g(b', \psi) = -(k_i - k_r) \cdot b + 2\eta_e(b').$$

Noting that

$$(k_i - k_r) \cdot b = -kb' \sin \theta \cos(\psi - \phi),$$

the stationary-phase conditions yield:

$$k \sin \theta \cos(\psi - \phi) + 2 \left(\frac{\partial \eta_e}{\partial b'} \right)_{b'} = 0,$$

$$-kb \sin \theta \sin(\psi - \phi) = 0,$$

where (b, φ) is the stationary-phase point.

The second equation gives directly $\phi = \varphi$. When this is substituted in the first, (12) is the result.

$g(b', \psi)$ in (10) is now expanded about the stationary-phase point (b, φ) . Noting that

$$\left(\frac{\partial^2 g}{\partial b' \partial \psi} \right)_{b, \varphi} = \left(\frac{\partial^2 g}{\partial \psi \partial b'} \right)_{b, \varphi} = 0,$$

the resulting integral is

$$f(\theta, \phi) = \frac{kb}{2\pi i} \exp[-ig(b, \varphi)] \int_0^{\infty} db' \exp \left[-\frac{1}{2} i \left(\frac{\partial^2 g}{\partial b'^2} \right)_{b, \varphi} (b' - b)^2 \right] \\ \times \int_0^{2\pi} d\psi \exp \left[-\frac{1}{2} i \left(\frac{\partial^2 g}{\partial \psi^2} \right)_{b, \varphi} (\psi - \varphi)^2 \right].$$

Changing to the variables x and y , which are related to b and ψ according to

$$x = \left[\frac{1}{2} \left(\frac{\partial^2 g}{\partial b'^2} \right)_{b,\varphi} \right]^{\frac{1}{2}} (b' - b), \quad y = \left[\frac{1}{2} \left(\frac{\partial^2 g}{\partial \psi^2} \right)_{b,\varphi} \right]^{\frac{1}{2}} (\psi - \varphi),$$

we obtain the integral

$$f(\theta, \phi) = \frac{kb}{\pi i} e^{-i\varphi(b,\varphi)} \left[\left(\frac{\partial^2 g}{\partial b'^2} \right)_{b,\varphi} \left(\frac{\partial^2 g}{\partial \psi^2} \right)_{b,\varphi} \right]^{-\frac{1}{2}} \\ \times \int_{x(0)}^{\infty} dx \exp[-ix^2] \int_{y(0)}^{y(2\pi)} dy \exp[-iy^2].$$

Replacing the integrals by their zero-order approximations $\pi^{\frac{1}{2}} e^{i\pi/4}$, and noting that

$$\left(\frac{\partial^2 g}{\partial b'^2} \right)_{b,\varphi} = \pm k \cos \theta \frac{\partial \theta}{\partial b} \quad \text{and} \quad \left(\frac{\partial^2 g}{\partial \psi^2} \right)_{b,\varphi} = \pm kb \sin \theta,$$

$f(\theta, \phi)$ can be expressed as*

$$f(\theta, \phi) = \left(\frac{b}{\sin \theta} \frac{\partial b}{\partial \theta} \right)^{\frac{1}{2}} e^{i\gamma_e},$$

where γ_e is a phase factor.

Then multiplying with its complex conjugate and using the semiclassical equivalence this results in (13).

II. *Nonspherically symmetric case.* The stationary-phase conditions are that now η_e is dependent on b' and ψ

$$k \sin \theta \cos(\varphi - \phi) + \left(\frac{\partial \eta_e}{\partial b'} \right)_{b,\varphi} = 0,$$

$$kb \sin \theta \sin(\varphi - \phi) + \left(\frac{\partial \eta_e}{\partial \psi} \right)_{b,\varphi} = 0.$$

Solving these equations for θ and ϕ yields (14a) and (14b).

* Note that in the small-angle range has been used $\sin \theta \approx \theta$ and $\cos \theta \approx 1$.

The integrand is, as in the spherically symmetric case expanded about its point of stationary phase. The cross term, however, does not vanish, so that the integrals over b' and φ do not uncouple. By choosing the new variables

$$p = \left[\frac{1}{2} \left(\frac{\partial^2 g}{\partial b'^2} \right)_{b,\varphi} \right]^{\frac{1}{2}} (b' - b) + \left[\frac{1}{2} \left(\frac{\partial^2 g}{\partial \varphi^2} \right)_{b,\varphi} \right]^{\frac{1}{2}} (\varphi - \varphi),$$

$$q = \left[\frac{1}{2} \left(\frac{\partial^2 g}{\partial b'^2} \right)_{b,\varphi} \right]^{\frac{1}{2}} (b' - b) - \left[\frac{1}{2} \left(\frac{\partial^2 g}{\partial \varphi^2} \right)_{b,\varphi} \right]^{\frac{1}{2}} (\varphi - \varphi),$$

the terms with the product $(b' - b)(\varphi - \varphi)$ cancel and the integral can be evaluated in the same way as in the spherically symmetric case. We obtain

$$f(\theta, \phi) = kb \exp [ig(b, \varphi)] \left[\left(\frac{\partial^2 g}{\partial b'^2} \right)_{b,\varphi} \left(\frac{\partial^2 g}{\partial \varphi^2} \right)_{b,\varphi} - \left(\frac{\partial^2 g}{\partial b' \partial \varphi} \right)_{b,\varphi}^2 \right]^{-1}.$$

Noting that

$$\left(\frac{\partial^2 g}{\partial b'^2} \right)_{b,\varphi} = \left(\frac{\partial^2 \eta_e}{\partial b'^2} \right)_{b,\varphi},$$

$$\left(\frac{\partial^2 g}{\partial b' \partial \varphi} \right)_{b,\varphi} = -k \sin \theta \sin (\varphi - \phi) + \left(\frac{\partial^2 \eta_e}{\partial b \partial \varphi} \right)_{b,\varphi},$$

$$\left(\frac{\partial^2 g}{\partial \varphi^2} \right)_{b,\varphi} = -kb \sin \theta \cos (\varphi - \phi) + \left(\frac{\partial^2 \eta_e}{\partial \varphi^2} \right)_{b,\varphi},$$

and using (14a) and (14b) the eikonal amplitude can be expressed as

$$f(\theta, \phi) = \frac{b}{\sin \theta} \left(\frac{\partial \theta}{\partial b} \frac{\partial \phi}{\partial \varphi} - \frac{\partial \theta}{\partial \varphi} \frac{\partial \phi}{\partial b} \right)^{-\frac{1}{2}} e^{i\delta_e},$$

where δ_e is a phase factor. Multiplying this expression with its complex conjugate and using the semiclassical equivalence yields (17).

REFERENCES

- 1) See for example, Landau, L.D. and Lifshitz, L.M., Quantum mechanics, Pergamon Press (London, 1959).
- 2) Eckart, C., Rev. mod. Phys. 20 (1948) 399.
- 3) Advances in chemical physics, Vol. X, Chapter 3, Intersc. Publishers Inc. (New York, London, Sydney, 1966) p. 95.
- 4) Glauber, R.J., Lectures in theoretical physics, Intersc. Publishers Inc. (New York, 1959) p. 331.

- 5) Joachain, C.J., private communication. See also Adachi, T. and Kotani, T., Progr. theor. Phys. **39** (1968) 430.
- 6) Cross Jr., R.J., J. chem. Phys. **46** (1967) 609.
- 7) Gradshteyn, I.S. and Ryzhik, I.M., Table of Integrals series and products, Academic Press (New York, London, 1965).
- 8) Franco, V. and Glauber, R.J., Phys. Rev. **142** (1195) 1966 appendix A.

IN HEADON COLLISIONS WITH He, U, AND D₂

M. VAN UPP, J. B. OVERBROEK and J. L. DE

Phys. Dept. of the Univ. of Groningen, Groningen, The Netherlands

Received 17 March 1971

Synopsis

Energy losses and deflection of K^+ ions having suffered a head-on collision with He, U, and D_2 . For K^+ ions of very small energy losses a characteristic energy range between 10 and 20 eV. Energy losses for this process are considered as a function of energy. From the energy dependence of the cross section the dependence of the scattering angle is investigated. Using an appropriate model, $\sigma(\theta) \sim \theta^{-2}$ is found to be 2.2 eV/deg. over the investigated range of scattering angles $0.1 < \theta < 10$ deg.

The collisions of K^+ with He, and U, show systematic energy losses due to vibrational excitation of the molecule. The experimentally observed energy losses are compared with calculations based on a model of a collision between a particle with a horizontal velocity v_{rel} and a molecule at rest. At higher energies there are deviations from the energy transfer, probably because of contributions of multiple collisions with the molecule or atoms. Above 10 eV, energy losses corresponding with molecular stripping collisions are also observed. For a better theoretical description a test of the calculated values must be made in experiments.

1. Introduction. In previous papers^{1,2} we describe the interaction of K^+ ions with noble gases confined strictly to forward-scattered ions. From these measurements the interaction potentials for the scattering of K^+ ions from atoms (previously determined, for only nuclear distances ranging from 1 to 3 Å).

This paper deals with backward-scattered K^+ ions. The results provide information about the interaction at smaller interaction distances. However, reliable processes can be observed by measuring the energy loss of the K^+ ions by means of mass spectroscopic analysis of the particle ion counters. These measurements are an extension of the work of other experimentalists^{3,4,5} and subject to the interest of theoretical investigators^{6,7}.

2. Experimental. For the description of the apparatus, we refer also to an earlier paper¹. An ion beam is produced by thermal ionization of K^+

of stationary phase. The cross term, however, is not stationary and is usually neglected. This is the case in the present case. The cross term, however, is not stationary and is usually neglected. This is the case in the present case.

$$p = \left[\frac{1}{2} \left(\frac{\partial^2 g}{\partial \theta^2} \right)_{\theta=\theta_0} \right]^{-1/2} \left[\frac{1}{2} \left(\frac{\partial^2 g}{\partial \phi^2} \right)_{\phi=\phi_0} \right]^{-1/2} \\ q = \left[\frac{1}{2} \left(\frac{\partial^2 g}{\partial \theta^2} \right)_{\theta=\theta_0} \right]^{-1/2} (\theta - \theta_0) - \left[\frac{1}{2} \left(\frac{\partial^2 g}{\partial \phi^2} \right)_{\phi=\phi_0} \right]^{-1/2} (\phi - \phi_0)$$

the terms with the product $(\theta - \theta_0)(\phi - \phi_0)$ cancel and the integral can be evaluated in the same way as in the spherically symmetric case. We obtain

$$f(\theta, \phi) = k^2 \exp [i\pi/4 (\theta - \theta_0)] \left[\left(\frac{\partial^2 g}{\partial \theta^2} \right)_{\theta=\theta_0} \left(\frac{\partial^2 g}{\partial \phi^2} \right)_{\phi=\phi_0} - \left(\frac{\partial^2 g}{\partial \theta \partial \phi} \right)_{\theta_0, \phi_0} \right]^{-1/2}$$

Noting that

$$\left(\frac{\partial^2 g}{\partial \theta^2} \right)_{\theta_0, \phi_0} = \left(\frac{\partial^2 g_0}{\partial \theta^2} \right)_{\theta_0} \\ \left(\frac{\partial^2 g}{\partial \theta \partial \phi} \right)_{\theta_0, \phi_0} = -\rho \sin \theta \sin (\phi - \theta) + \left(\frac{\partial^2 g_0}{\partial \theta \partial \phi} \right)_{\theta_0} \\ \left(\frac{\partial^2 g}{\partial \phi^2} \right)_{\theta_0, \phi_0} = -k^2 \sin^2 \theta \sin (\phi - \theta) + \left(\frac{\partial^2 g_0}{\partial \phi^2} \right)_{\theta_0}$$

and using (14a) and (14b) the diffracted amplitude can be expressed as

$$f(\theta, \phi) = \frac{2}{\sqrt{\sin \theta}} \left(\frac{\partial g_0}{\partial \theta} \frac{\partial g_0}{\partial \phi} - \frac{\partial g_0}{\partial \phi} \frac{\partial g_0}{\partial \theta} \right)^{-1/2} e^{i\delta}$$

where δ is a phase factor. Multiplying this expression with its complex conjugate and using the semiclassical equivalence yields (17).

REFERENCES

1. See for example, Lighthill, J. D., and Leiberman, L. M., *Wave Scattering*, Pergamon Press, London, 1963.
2. Yehou, C., *Rev. Mod. Phys.* **28** (1956) 36.
3. *Asymptotic Methods in Physics*, Vol. 2, (Chapman & Hall) Interscience Inc., New York, London, New York, 1962, p. 95.
4. Chao, K. S., *Journal of Mathematical Physics*, **10** (1969) 1479.

ENERGY-LOSS MEASUREMENTS OF K^+ IONS IN HEAD-ON COLLISIONS WITH He, H_2 AND D_2

H. VAN DOP, A. J. H. BOERBOOM and J. LOS

FOM-Instituut voor Atoom- en Molecuulfysica, Amsterdam, Nederland

Received 19 March 1971

Synopsis

Energy losses are determined of K^+ ions having suffered a head-on collision with He, H_2 and D_2 . For K^+ on He only elastic scattering is observed, in a laboratory energy range from 250 to 2500 eV. Cross sections for this process are measured as a function of energy. From the energy dependence of the cross section the steepness of the repulsive interaction potential is determined. Using an inverse-power model, $V(r) = K/r^s$, s is found to be 2.2 ± 0.2 , over the investigated range of interaction: $0.3 \text{ \AA} \leq r \leq 0.6 \text{ \AA}$.

The collisions of K^+ with H_2 and D_2 show inelastic energy losses due to vibrational excitation of the molecules. The experimentally observed inelastic energy transfer is compared with calculations based on a model of a collinear collision of a particle with a harmonic oscillator. Below 22 eV centre-of-mass energy there is a good agreement between theory and experiment. At higher energies theory predicts too low values for the energy transfer, probably because it overestimates the importance of multistep collisions with the harmonic oscillator. Above 26 eV, energy losses corresponding with impulsive stripping collisions are also observed. For a better theoretical description a two- or three-dimensional collision model should be used in our opinion.

1. *Introduction.* In previous papers^{1,2}) we described the interaction of K^+ ions with noble gases confining ourselves to forward-scattered ions. From these measurements the interaction potentials for the scattering of K^+ ions from noble gases were determined, for internuclear distances ranging from 1 to 3 \AA .

This paper deals with backward-scattered K^+ ions. The results provide information about the interaction at smaller internuclear distances. Moreover, inelastic processes can be observed by measuring the energy loss of the K^+ ions by means of mass-spectrometric analysis of the particle momentum. These measurements are an extension of the work of other experimentalists^{3,7,8,9}) and subject to the interest of theoretical investigators^{4,5,6}).

2. *Experimental.* For the description of the apparatus we may refer to an earlier paper¹). An ion beam is produced by thermal ionization of KCl.

After acceleration and collimation the beam passes through a 0.7 cm long collision chamber filled with gas. The scattered beam is collimated, energy analyzed and detected. The energy analysis is performed by means of a mass spectrometer with an energy resolution of about 1 : 50. This resolution makes it possible to separate the forward-scattered and the nonscattered ions from those scattered backwards, the latter having lost a considerable amount of energy.

In order to determine the energy loss accurately the magnetic field of the analyzer magnet was held fixed on a suitable value and the accelerating voltage was scanned. In this way it is possible to make an energy-loss spectrum of the scattered beam. This procedure provides a direct measure of the energy loss in eV.

3. *Results.* We started with measurements of K^+ ions on He. Simultaneously energy loss and relative intensity of the head-on collided K^+ ions was measured. In the laboratory frame of reference the cross section for elastic head-on collisions is given by (see appendix):

$$\sigma_{bs}(\theta_0, E) = i \frac{\sigma(\theta_0, E - \Delta E) - \sigma(\theta_0, E)}{\exp[-n\sigma(\theta_0, E)l] - \exp[-n\sigma(\theta_0, E - \Delta E)l]}, \quad (1)$$

where

- $\sigma_{bs}(\theta_0, E)$ is the total incomplete cross section for a head-on collision at an energy E (resulting in an energy loss ΔE),
- $\sigma(\theta_0, E)$ the attenuation cross section for ions with an energy E ,
- n the particle density of the target gas in the collision chamber,
- l the length of the collision chamber,
- i the intensity of the head-on collided particles relative to that of the primary beam.

i was determined by measuring the peak height of the backward-scattered ions, relative to the peak height of the primary beam which was determined with an evacuated collision chamber. The primary beam, however, has an energy, which is different from the energy of the head-on collided particles. As the gain of the multiplier is a function of the particle energy, we have to apply a correction in order to obtain the correct ratio between the two intensities. This correction was determined by calibrating the multiplier gain with a known beam current.

For the evaluation of $\sigma_{bs}(\theta_0, E)$, the attenuation cross sections $\sigma(\theta_0, E)$ must be known as functions of energy. The values of these cross sections were determined in an earlier stage. They have been tabulated in ref. 2.

First the pressure dependence of i was checked. The result is given in fig. 1. According to (1) i must have a maximum value, which appears (*cf.*

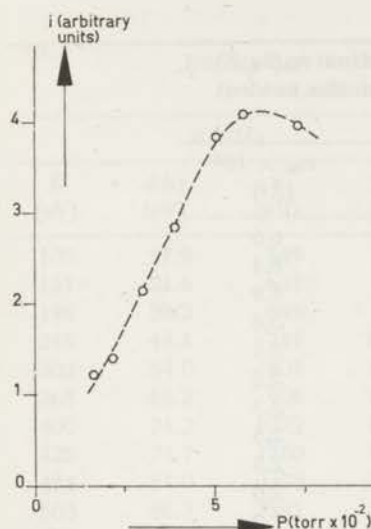


Fig. 1

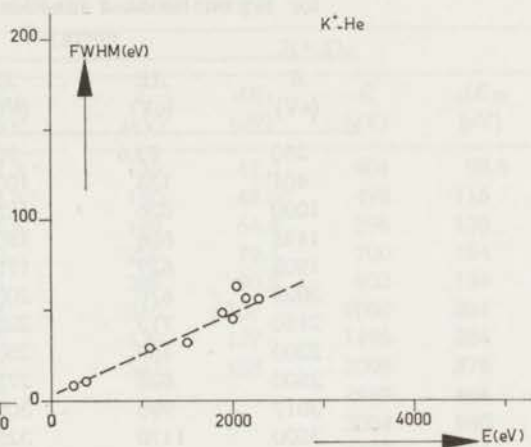


Fig. 2

Fig. 1. The intensity of the head-on scattered K⁺ ions as a function of the pressure of the target gas (He) at 3000 eV.

Fig. 2. The full width half maximum of the peak, resulting from head-on collisions of K⁺ ions with He as a function of the incident energy.

fig. 1) at a pressure of about 6.5×10^{-2} torr. Differentiating i with respect to p , and finding the value of p at which i has an extremum yields $p = 9.6 \times 10^{-2}$ torr. This is in rather fair agreement with the experimentally obtained value, taking into account the rather crude measurement of the pressure. As working pressure we took the value of p for which i was optimal *i.e.* about 5×10^{-2} torr. It should be noted here that in the derivation of (1) it is assumed that the attenuation of the primary beam is linearly dependent on pressure. This means that the validity of (1) has an upper limit in the pressure range. In a previous paper¹⁾ the linearity of the attenuation was tested. From these measurements we may conclude that for a pressure of 5×10^{-2} torr the linearity still holds within a few percent, so that formula (1) may be used without making large errors. The results of the K⁺-He cross section and energy-loss measurements are given in table I. For the calculation of the energy losses the energy corresponding with the top of the peak was determined. In order to check the peak shape over the investigated energy range, the fwhm (full width half maximum) was measured (*cf.* fig. 2). Up to 2500 eV the fwhm was linear with energy and in agreement with the resolution of the apparatus. Above 2500 eV peak broadening occurs and at 4000 eV, a shoulder of a second peak is observed, probably due to electronic excitation. Peak broadening due to thermal

TABLE I

Energy loss (ΔE) and cross section $\sigma_{bs}(\theta_0, E)$ for K^+ on He as a function of the incident energy E			
E (eV)	ΔE (eV)	E (eV)	$\sigma_{bs} \times 10^4$ (\AA^2)
250	83.6	750	6.6
401	135	1000	5.4
1000	336	1250	4.9
1496	506	1500	3.8
1905	629	1750	3.5
2024	676	2000	2.8
2150	713	2250	3.3
2300	763	2500	2.5
2500	828	2750	2.5
3017	998	3000	2.0
3500	1170	3250	1.9
4000	1329	3500	1.6
		3750	1.6
		4000	1.5

motion of the target is estimated to be less than 5% of the total width and can be neglected.

For the combinations K^+-H_2 and K^+-D_2 two peaks were observed in the investigated energy range. The lower energy limit was determined by the intensity of the primary beam, which decreases very fast below 150 eV. At about 550 eV for H_2 and 400 eV for D_2 a second peak was observed (*cf.* fig. 3), while the intensity of the first one decreased and finally disappeared

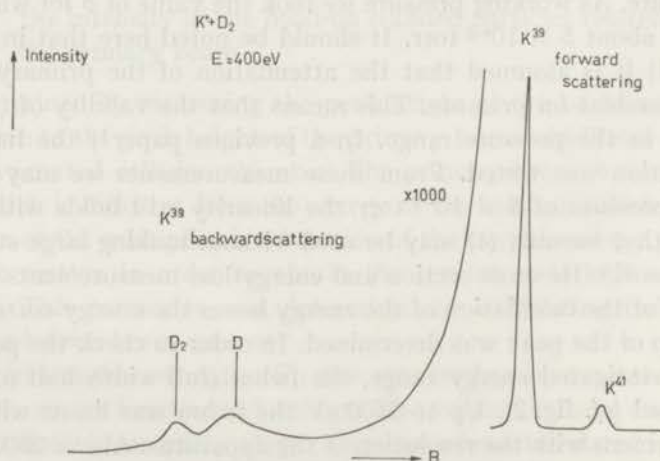


Fig. 3. Energy analysis of the scattered signal. The peak marked D_2 corresponds with the collinear model; the peak marked D with the stripping model.

TABLE II

Energy loss for the combinations K ⁺ -H ₂ and K ⁺ -D ₂ as a function of the incident energy							
K ⁺ -H ₂				K ⁺ -D ₂			
<i>E</i> (eV)	ΔE_I (eV)	<i>E</i> (eV)	ΔE_{II} (eV)	<i>E</i> (eV)	ΔE_I (eV)	<i>E</i> (eV)	ΔE_{II} (eV)
100	17.9	549	77.2	130	41.3	401	98.8
121	21.6	607	84.8	150	48.6	498	115
194	35.3	698	95.5	199	64.8	596	135
245	44.4	749	100	250	79.4	700	154
303	54.0	804	105	295	90.8	803	184
365	65.2	908	114	350	107	1000	201
400	71.2	1022	130	429	127	1496	284
425	74.7	1750	193	541	158	2005	375
474	81.0	2370	242			2498	464
503	86.3	2891	287			3004	560
537	90.7	3419	339			3493	654
565	94.6	3924	387			3950	730
600	99.4						
650	106						
719	116						
774	125						
831	133						

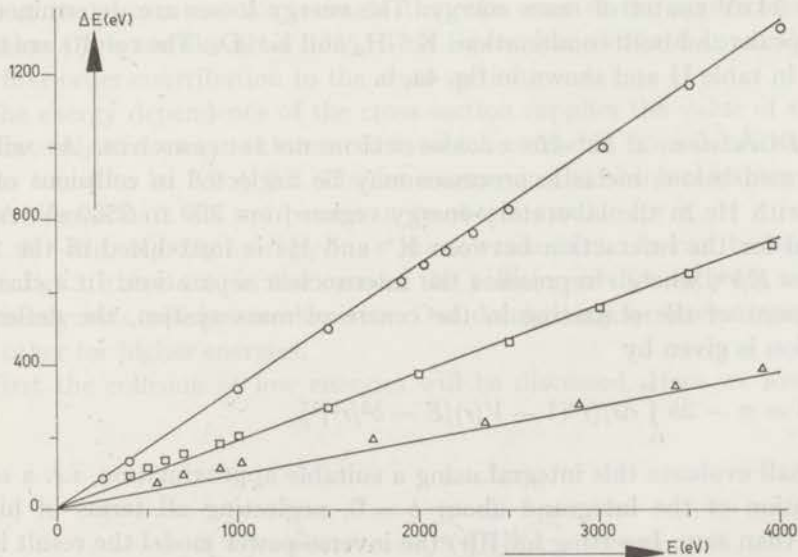


Fig. 4a. Energy loss ΔE as a function of the primary energy E in the laboratory frame for the combinations K⁺-He (\circ), K⁺-H₂ (Δ , \blacktriangle) and K⁺-D₂ (\square , \blacksquare). The solid lines correspond with eq. (12).

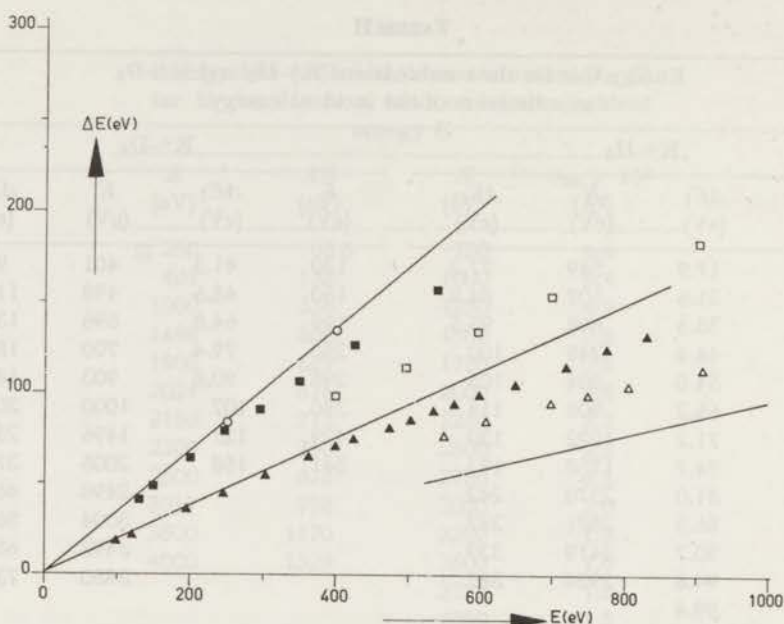


Fig. 4b. Detail of fig. 4a.

at about 830 and 540 eV for H_2 and D_2 , respectively. The threshold for the appearance of the second peak (which should be the same for H_2 and D_2 when the collision is considered in the centre of mass system) is estimated to be 24 eV centre of mass energy. The energy losses are determined for both peaks and both combinations K^+-H_2 and K^+-D_2 . The results are tabulated in table II and shown in fig. 4a, b.

4. Discussion. a. K^+-He cross-section measurements. As will be confirmed below, inelastic processes may be neglected in collisions of K^+ ions with He in the laboratory-energy region from 750 to 2500 eV. A potential for the interaction between K^+ and He is introduced of the form $V(r) = K/r^s$, where r represents the internuclear separation. In a classical treatment of the scattering in the centre of mass system, the deflection function is given by

$$\theta = \pi - 2b \int_{r_0}^{\infty} dr / [r^2(1 - V(r)/E - b^2/r^2)^{1/2}]. \quad (2)$$

We shall evaluate this integral using a suitable approximation, *i.e.* a series expansion of the integrand about $b = 0$, neglecting all terms of higher order than zero. Inserting for $V(r)$ the inverse power model the result is

$$\theta = \pi - 2b(K/E)^{-1/s} \pi^{1/2} [\Gamma(1 + 1/s) / \Gamma(\frac{1}{2} + 1/s)], \quad (3)$$

where $\Gamma(x)$ is the complete gamma function. Now introducing the classical

differential cross section for scattering of K⁺ from He, in the centre of mass system:

$$\frac{d\sigma}{d\Omega} = - \frac{b}{\sin \theta} \frac{db}{d\theta}, \quad (4)$$

the cross section for backward scattering $\sigma_{bs}(\theta, E)$ between the angles π and $\pi - \theta$ ($\theta \ll 1$) results from the integration:

$$\sigma_{bs}(\theta, E) = 2\pi \int_{\pi-\theta}^{\pi} \frac{d\sigma}{d\Omega} \sin \theta' d\theta'. \quad (5)$$

Substituting (4) yields

$$\sigma_{bs}(\theta, E) = \pi b^2(\pi - \theta, E). \quad (6)$$

As $b(\pi - \theta, E)$ is known from (3) we get after transforming to the laboratory system

$$\sigma_{bs}(\theta_0, E) = \pi \left\{ \frac{m_1 - m_2}{m_2} \right\}^2 \left\{ \frac{m_2}{m_1 + m_2} \right\}^{-2/s} [\theta_0 / 2g(s)]^2 (K/E)^{2/s}, \quad (7)$$

where m_1 and m_2 is the mass of the projectile and the target particle, respectively, and

$$g(s) = \pi^{1/2} \Gamma(1 + 1/s) / \Gamma(\frac{1}{2} + 1/s).$$

The accuracy of this expression depends of course on the values of b which are contributing to the scattering and, consequently, on the angular aperture of the apparatus. We estimate that the error of the approximate expression (7) is smaller than 15%. This figure was obtained by evaluating the first-order contribution to the cross section.

The energy dependence of the cross section supplies the value of s . Over the investigated range of interaction, which extended from 0.3 Å to 0.6 Å, s was found to be 2.2 ± 0.2 . The inaccuracy in the absolute values of the experimental data did not permit us to obtain a value for K .

b. K⁺-He, H₂, D₂ energy-loss measurements. As can be observed from fig. 3, there are, in the case of the collision of K⁺ with H₂ and D₂, obviously two collision mechanisms: One dominating for low energies, and the other for higher energies.

First the collision at low energies will be discussed. Here we assume a

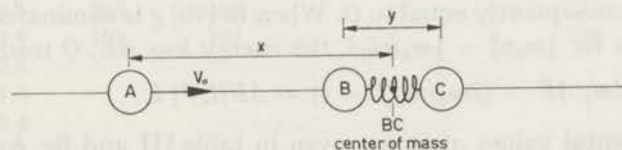


Fig. 5. Coordinates for a collinear collision of a particle A with a harmonic oscillator BC.

collinear collision of a particle A with a harmonic oscillator BC (representing the diatomic molecule). Further it is assumed that A only interacts with B (*cf.* fig. 5). When B is rigidly bonded to C the collision can only be purely elastic, if we neglect electronic excitation. The energy loss ΔE of the projectile, can be obtained by solving the equations of conservation of momentum and energy, and is given by

$$\Delta E = (4m_a m / M^2) E, \quad (8)$$

where $M = m_a + m_b + m_c$, $m = m_b + m_c$ and E is the primary energy in the laboratory system. The solid lines in fig. 4a, b correspond with this formula, where m was taken to be 4, 2, and 1, respectively. (It is clear that the elastic collision between K^+ and He will satisfy (8), when we substitute $m = 4$.) The measure of inelasticity appears by the deviation of the experimental data from these lines. As we see in fig. 4a, inelastic energy losses do not occur in collisions of K^+ on He up to 2500 eV laboratory energy. This means that, in agreement with our expectations, electronic excitation (or ionization) of target or projectile can be neglected at low velocities ($\lesssim 10^5$ m/s). Without speculating too much we may suppose that for K^+ on H_2 and D_2 these processes also can be neglected below 2500 eV. In fig. 4b we see that the deviations from the "elastic" lines for H_2 and D_2 already occur at low energies, apparently due to mainly vibrational excitation, rotational excitation being improbable in head-on collisions. These deviations are caused by inelastic energy transfer to the diatomic molecule. We shall now convert ΔE , the energy loss in the laboratory frame, to Q , the energy of internal motion of BC, which quantity suits better for theoretical discussion. When v_0 is the laboratory velocity of A, and the molecule BC is stationary, we have the conservation laws

$$\begin{aligned} \frac{1}{2} m_a v_0^2 &= \frac{1}{2} m_a (v'_0)^2 + \frac{1}{2} m_b v_b^2 + \frac{1}{2} m_c v_c^2 \\ m_a v_0 &= m_a v'_0 + m_b v_b + m_c v_c. \end{aligned} \quad (9a)$$

As only particles are detected which are scattered through angles smaller than 2.6×10^{-3} rad, the component of v'_0 perpendicular to v_0 is neglected, giving

$$\frac{1}{2} m_a v_0^2 = \frac{1}{2} m_a (v'_0)^2 + \frac{1}{2} \mu \dot{y}^2 + \frac{1}{2} m g^2, \quad m_a v_0 = m_a v'_0 + m g, \quad (9b)$$

where μ is the reduced mass, \dot{y} the relative velocity and g the centre of mass velocity of B and C. The kinetic energy, $\frac{1}{2} \mu \dot{y}^2$, is the energy of internal motion and consequently equal to Q . When in (9b) g is eliminated, and when we substitute for $\frac{1}{2} m_a v_0^2 - \frac{1}{2} m_a (v'_0)^2$, the energy loss ΔE , Q reads:

$$Q = (M/m) \Delta E - (2m_a/m) [1 - (1 - \Delta E/E)^{\frac{1}{2}}] E. \quad (10)$$

The experimental values of Q are given in table III and fig. 6. The values Q_I and Q_{II} correspond to the energy losses ΔE_I and ΔE_{II} , respectively.

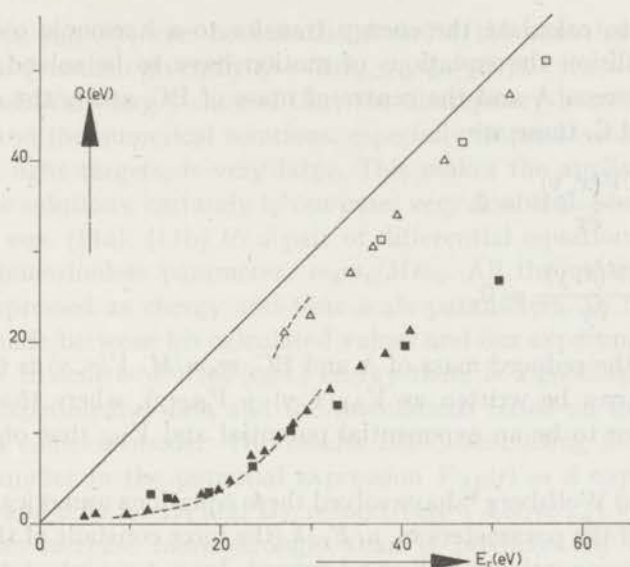


Fig. 6. Inelastic energy transfer to the molecule, Q , as a function of the centre-of-mass energy E_c .

K^+-H_2 (Δ , \blacktriangle) (this work)
 K^+-D_2 (\square , \blacksquare) (this work)
 K^+-D_2 (---) (Dittner and Datz³)
 The solid line corresponds with eq. (14).

TABLE III

Inelastic energy loss (Q) as a function of the centre-of-mass energy for the combinations K^+-H_2 and K^+-D_2

H_2				D_2			
$E_{c.m.}$ (eV)	Q_I (eV)	$E_{c.m.}$ (eV)	Q_{II} (eV)	$E_{c.m.}$ (eV)	Q_I (eV)	$E_{c.m.}$ (eV)	Q_{II} (eV)
4.93	0.8	27.0	21.2	12.2	3.2	37.6	31.3
5.96	1.2	29.8	23.1	14.1	2.7	46.6	42.2
9.55	1.1	34.3	27.7	18.7	3.3	55.8	51.1
12.0	1.5	36.8	30.6	23.4	6.3	65.6	61.7
14.9	2.7	39.5	34.1	27.6	10.1	84.6	82.7
18.0	3.3	44.7	40.2	32.8	13.2	93.7	92.0
19.7	3.9	51.9	47.4	40.2	19.6	140	140
20.9	4.9	86.1	83.9	50.7	26.6	188	187
23.3	7.6	117	116			234	234
24.8	7.9	142	142			281	281
26.4	9.6	168	168			327	326
27.8	10.9	193	193			370	370
29.5	12.5						
32.0	14.8						
35.4	17.4						
38.1	18.7						
40.9	21.3						

In order to calculate the energy transfer to a harmonic oscillator in a collinear collision the equations of motion have to be solved. If x is the distance between A and the centre of mass of BC, and y the distance between B and C, these are

$$m\ddot{x} + \frac{\partial V(x, y)}{\partial x} = 0, \quad (11a)$$

$$\mu\ddot{y} + \frac{\partial V(x, y)}{\partial y} = 0, \quad (11b)$$

where m is the reduced mass of A and BC, $m_a m/M$. $V(x, y)$ is the total potential and can be written as $V_{AB}(x, y) + V_{BC}(y)$, where that of V_{AB} is usually taken to be an exponential potential and V_{BC} that of a harmonic oscillator.

Kelley and Wolfsberg⁴) have solved these equations numerically, for various values of the parameters m , μ , E_r , k (the force constant of the molecule) and for an exponential as well as a Lennard-Jones-type interaction between A and B. Unfortunately, the mass combinations corresponding to our experiments were not included in their calculations, and their energy range was limited. An approximate analytical solution of eqs. (11a, b) is obtained by setting y equal to a constant value y_0 ⁵). By putting in eq. (11a) $V(x, y)$

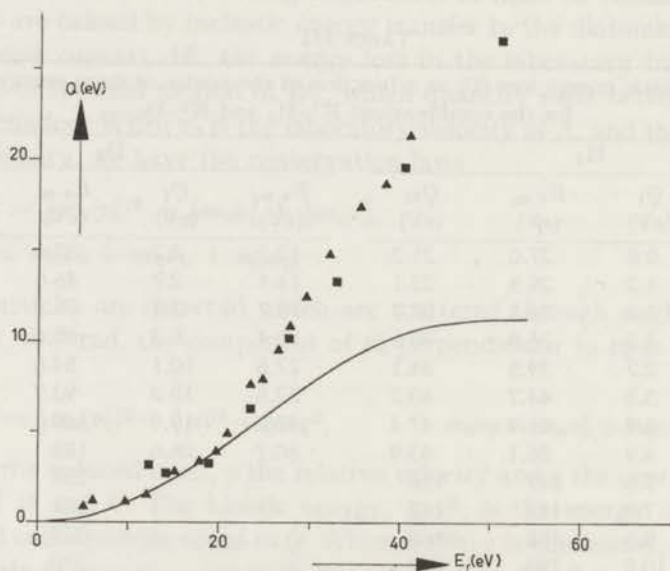


Fig. 7. Inelastic energy transfer to the molecule, Q_1 , as a function of the centre-of-mass energy E_r .

K⁺-H₂ (▲) (this work)

K⁺-D₂ (■) (this work)

K⁺-H₂, D₂ (—) (Secret⁶)

equal to $V(x, y_0)$, $x(t)$ can be calculated and (11b) can then be solved, yielding $y(t)$. Q is then given by $Q = \lim_{t \rightarrow +\infty} \frac{1}{2}\mu[\dot{y}(t)]^2$.

Kelley and Wolfsberg⁴⁾ showed that the discrepancy between these approximate and the numerical solutions, especially in the case of heavy projectiles and light targets, is very large. This makes the application of the approximate solutions, certainly in our case, very doubtful. Secrest⁶⁾ transformed the eqs. (11a), (11b) to a pair of differential equations containing only one dimensionless parameter: $m_a m_c / M m_b$. All the other parameters could be expressed as energy and time scale parameters. In fig. 7 a comparison is made between his calculated values and our experimental values. Up to 22 eV in centre-of-mass (c.m.) energy there is a good agreement between the experimental data and the calculations based on the plain one-dimensional collision model. The results fitted best using for L , the potential parameter in the potential expression $V_{AB}(r) = A \exp[-r/L]$, the values 0.30 and 0.33 for H₂ and D₂, respectively[†]. Above 22 eV the inelastic energy losses increase more strongly than is predicted by theory. Our measurements, however, agree fairly well with those of Dittner and Datz³⁾ (cf. fig. 6), which is a strong argument for the correctness of the experimental data, the more as the experimental techniques used by them were quite different from ours. We may conclude that the collinear model predicts too low values for Q at higher energies. This discrepancy is readily clarified when A, B and C are considered to be rigid spheres. In a collinear collision A will transfer an amount of energy to B, which in turn transfers (part of) it to C. If $m_b = m_c$, B will be at rest after this last step. A, however, still has forward momentum if $m_a > m_b$, and will collide once more with B. Such a sequence strongly reduces the internal energy of BC. In the actual experiment, however, most collisions are not exactly collinear, and in these the above loss of internal energy will not be nearly as efficient. As a result, the amount of internal energy of BC predicted by the collinear model will be smaller than that found experimentally. What happens in a soft collision is more difficult to discuss but it may be apparent that calculations for soft interactions in the high-energy limit will approach the rigid-sphere case. For a more extensive discussion we may refer to ref. 6. Above 40 eV c.m. energy the intensity of the collisions of the type discussed above strongly decreases, suggesting that a "better" collinearity is required at higher energies.

While the intensity of the first peak is diminishing a second peak is observed at about 26 eV c.m. energy. This suggests that a second collision process is appearing which essentially cannot be explained with the collinear model. For this second process a stripping collision is proposed: In a

[†] Note added in proof.

The value 0.33 for L is in striking agreement with the value 0.320 predicted by Amdur for the system K⁺-D₂ (cf. ref. 9).

(non-collinear) collision, a K^+ ion has an impulsive head-on collision with one of the atoms of the molecule, while the other atom is a "spectator" of the collision. The "spectator" atom interacts only *via* the molecular bonding. The bond becomes negligible when the energy of motion highly exceeds the bonding energy. In the limiting case of vanishing molecular bond the energy loss of the primary particle is simply:

$$\Delta E = [4m_a m_b / (m_a + m_b)^2] E. \quad (12)$$

This amount of energy is transferred only to atom B of the molecule. When the initial energy of the molecule BC is zero, then the final energy of BC in its own centre of mass system, Q is given by

$$Q = [4m_a \mu / (m_a + m_b)^2] E, \quad (13)$$

or using E_r , the total energy in the centre of mass system:

$$Q = \{4m_a \mu M / [(m_a + m_b)^2 m]\} E_r. \quad (14)$$

We observe that for higher energies the H_2 and D_2 measurements corresponding with the energy losses ΔE_{II} indeed converge to (12), taking for m_b the masses 1 and 2 respectively. The solid line in fig. 6 corresponds with formula (14). We should expect from (14) two straight lines with different slopes, corresponding to the masses of H and D. The difference between the slopes, however, is negligible so that we have only drawn one line for both H and D. The values of Q_{II} converge to this line when the energy increases, in agreement with the convergence of ΔE_{II} to the lines given by eq. (12). Dittner and Datz³) have suggested that this second peak is due to a dissociative excitation of the molecule for an $n = 1$ to $n = 2$ transition in D_2 (or H_2). The experimental data can, as is shown, also be interpreted using the stripping model [eq. (12), fig. 4a]. In order to have more convincing arguments for this model we performed the following experiment[†]: High-energy Ar^+ ions (10 keV) were scattered on HD. As a consequence of this model we should see two different peaks corresponding to an energy loss in a collision with an H and D atom, respectively. This was verified by the experiment. When H_2 and D_2 were used as target gas, the peak corresponding to the energy loss of the alternate isotope disappeared. With this experiment it is proved that at high energies only one of the atoms of the molecule is involved in the collision. Whether the collision is exclusively impulsive or simultaneous electronic excitation has to be taken into consideration could not be determined experimentally. Cheng *et al.*⁷) did an experiment using molecular ions as projectiles and He as target gas. They determined the velocity distribution of the ionic fragment which resulted

[†] For this experiment another (but similar) apparatus was used, as the original apparatus already was dismantled.

from the collision. The assumption of a purely impulsive stripping collision, however, is contradicted by their experiments. They propose a stripping collision mechanism in which the target atom and one of the atoms of the molecule adiabatically produce a short-lived collision complex with electronic properties such that the bonding between the two atoms of the molecule is greatly diminished. They found some experimental evidence for this model.

We may conclude that for a complete theoretical description of these collision phenomena a two- or three-dimensional collision model should be used, in order to circumvent the difficulty of the multi-step collisions in the one-dimensional model. A higher-dimensional model would also give a quantitative description of the deviation at lower energies of ΔE_{II} from the solid line (*cf.* figs. 4 and 6) which corresponds with the stripping collision.

Acknowledgements. The authors are indebted to Dr. T. R. Govers for his comments on the manuscript, and to R. Geutskens for his assistance in the measurements.

This work is part of the research program of the Stichting voor Fundamenteel Onderzoek der Materie (Foundation for Fundamental Research on Matter) and was made possible by financial support from the Nederlandse Organisatie voor Zuiver-Wetenschappelijk Onderzoek (Netherlands Organization for the Advancement of Pure Research).

APPENDIX

In order to derive from the measured intensity the cross section $\sigma_{bs}(\theta_0, E)$ for a head-on collision we make the following assumptions.

We assume that only elastic scattering processes occur in the collision chamber. Further, the cross section for a head-on collision is much smaller than that for a glancing collision: $\sigma_{bs}(\theta_0, E) \ll \sigma(\theta_0, E)$. When we consider an infinitesimal line element of length dx in the collision region parallel to the beam direction, then we may write for the change in intensity $di(x)$ of particles which have a head-on collision

$$di(x) = n\sigma_{bs}I(x) dx - n\sigma'i(x) dx, \quad (15)$$

where $i(x)$ is the intensity of head-on collided particles, n the target particle density, σ_{bs} the cross section for a head-on collision, σ' the attenuation cross section for particles which already have suffered a head-on collision. The prime denotes that this cross section has to be evaluated at an energy $E - \Delta E$, where E is the primary energy and ΔE the (elastic) energy loss corresponding with the head-on collision. When $\sigma_{bs} \ll \sigma$ then $I(x)$, the intensity of the primary beam at distance x from the entrance of the collision

chamber, is given by

$$I(x) = I(0) \exp(-n\sigma x).$$

Substituting $I(x)$ in (15) gives a differential equation of the form

$$y' - by = a \exp(-\alpha x),$$

the solution of which is well known. If the collision chamber has length l , σ_{bs} is given by

$$\sigma_{bs} = \frac{i}{I(0)} (\sigma' - \sigma) / [\exp(-n\sigma l) - \exp(-n\sigma' l)],$$

which, taking into account a correction for the multiplier gain, leads to eq. (1).

REFERENCES

- 1) Amdur, I., Inouye, H., Boerboom, A. J. H., Steege, A. N. v. d., Los, J. and Kistemaker, J., *Physica* **41** (1969) 566.
- 2) Boerboom, A. J. H., van Dop, H. and Los, J., *Physica* **46** (1970) 458.
- 3) Dittner, P. F. and Datz, S., *J. chem. Phys.* **49** (1968) 1969.
- 4) Kelley, J. D. and Wolfsberg, M., *J. chem. Phys.* **44** (1965) 324.
- 5) Rapp, D. and Kassal, T., *Chem. Rev.* **69** (1969) 61.
- 6) Secrest, D., *J. chem. Phys.* **51** (1969) 421.
- 7) Cheng, M. H., Chiang, M., Gislason, L. A., Mahan, B. H., Tsao, C. W., Werner, A. S., *J. chem. Phys.* **52** (1970) 5518.
- 8) Schöttler, J. and Toennies, P. J., to be published.
- 9) Dittner, P. F. and Datz, S., *J. chem. Phys.* **54** (1970) 4228.

CALCULATIONS ON ENERGY TRANSFER TO A DIATOMIC MOLECULE IN HIGH ENERGY HEAD-ON COLLISIONS

H. VAN DOP, A.J.H. BOERBOOM and J. LOS

FOM-Instituut voor Atoom- en Molecuulfysica, Amsterdam, Nederland

Synopsis

In collisions where the incident particle has zero impact parameter with respect to one of the atoms of the molecule the energy transfer and the scattering angle are calculated as a function of energy and molecular orientation. The interaction between the atoms of the molecule and the incident particle is described by an exponential potential. Three intramolecular potentials are used: a harmonic, a Morse and a modified Buckingham potential. No important differences are found in the results of the application of the last two potentials. At low energies the energy-transfer data and (laboratory) small-angle scattering data show that the molecule, in its totality, is involved in the collision. When the energy is increased only one atom of the molecule is involved in the collision, while the other is "watching" the collision. These so-called "stripping" or "spectator" collisions reveal, as it were, the mass structure of the molecule.

Finally some experimental data are discussed in connection with this collision model.

1. *Introduction.* In the last few years many calculations have been done on energy transfer in collisions of an atom with a diatomic molecule^{1,2,3,4}). One usually assumes in these collisions a collinear configuration (fig. 1a); the atoms b and c of the molecule are harmonically bound, and a interacts only with the near-

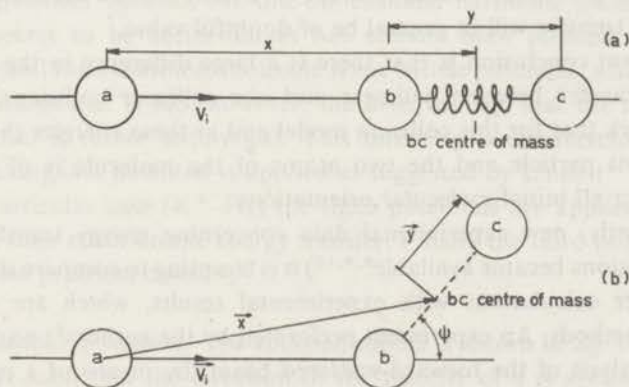


Fig. 1. a) Coordinates for a collinear collision of particle a with a harmonic oscillator bc.
b) Two-dimensional collision model.

by atom of the molecule (b). The interaction between a and b is generally described by an exponential potential. Quantum-mechanical^{2,4)} as well as classical¹⁾ or semiclassical^{3,5)} calculations have been done. A comparison is made by Heidrich *et al.*⁵⁾ among the various types of calculations, and we may conclude that in general there is good agreement among them. For some approximate calculations, however, exceptions have to be made. For example, when the collision energy approaches the zero-point energy of the harmonic oscillator, the (semi)classical approximation fails. A second approximation, which is widely used, is setting the intramolecular coordinate $y(t)$ equal to a constant during the collision. The equation of motion is then easily solved, and one ends up with an analytical expression for the energy transfer. This approximation overestimates the energy transfer, for values of the mass parameter $m = m_a m_c / (m_a + m_b + m_c) m_b$ larger than about 0.1. Mahan⁶⁾ improved the approximation by adjusting the reduced masses in the equations of motion in order to get the right asymptotic behaviour, when the collision energy, measured in units of the zero-point energy of the diatomic molecule, tends to infinity. This improvement ("the refined impulse approximation") led to an expression of increased accuracy. For values of $m \gtrsim 0.5$ the approximation deviates, however, from the exact result.

In a paper by Kelly and Wolfsberg⁷⁾ a two-dimensional collision model was introduced, on which they carried out their calculations. Most of their discussion is confined to zero-impact parameter collisions, by which they mean that the relative a-bc velocity vector is pointing toward the centre-of-mass of the molecule. They calculated rotational and vibrational energy transfer at 0.5, 0.75, 1 and 2 eV. From their calculations concerning rotational-energy transfer, they concluded that rotational-energy transfer can be adequately described by taking the molecule to be a rigid rotator. From the examination of the vibrational-energy transfer as a function of molecular orientations they conclude that the introduction of a steric factor in a collision model in order to obtain a more accurate description of the energy transfer will in general be of doubtful value.

An important conclusion is that there is a large difference in the efficiency of the energy transfer between collinear and non-collinear collisions. Finally we want to remark that for this collision model and at these energies the interaction of the incident particle and the two atoms of the molecule is of about equal importance for all initial molecular orientations.

Since, recently, new experimental data concerning energy transfer in atom-molecule collisions became available^{8,9,10)} it is tempting to compare the theoretical energy-transfer calculations with experimental results, which are obtained by using beam methods. An experiment performed by the authors⁸⁾ was based upon an energy analysis of the forward-scattered beam, by means of a mass spectrometer. Measurements on $K^+ - H_2$ and $K^+ - D_2$ were carried out for centre-of-mass energies ranging from 5 to 370 eV. Others^{9,10)} investigated $Li^+ - H_2$; K^+ , $K^0 - H_2$, D_2 ; $Na^+ - H_2$, D_2 and $Na^+ - H_2$, using time-of-flight techniques. One of the

striking features which as yet have not been explained by theory is the appearance at high energies of double energy-loss peaks in the energy spectrum of the scattered beam. These have to be ascribed to the fact that at higher energies the molecule behaves more and more like two separate particles. Further, the energy transfer as predicted by the collinear model is lower than is observed experimentally. This discrepancy does not seem to be removed by carrying out a two- or three-dimensional calculation⁹).

In the present paper the authors will try to get a better understanding of the experimental data. For this purpose the one-dimensional model is extended, so that it is in better agreement with the physical situation. In the extended model the one-dimensional constraint will be removed. Moreover we have applied more realistic intramolecular potentials, which can also account for molecular dissociation.

2. *The collision model.* In the extended model we shall consider for simplicity zero-impact parameter two-dimensional collisions, as we only want to illustrate some aspects of the experiments done in this field. Here we understand by zero-impact parameter collisions that the incident direction of the projectile (a) is pointing into the direction of one of the atoms (b) of the molecule (*cf.* fig. 1b). For high energies this will be a reasonable assumption, as the distance of closest approach of the projectile to one of the atoms of the molecule will be small compared with the molecular internuclear distance.

The intra-molecular interaction is represented by the harmonic potential, the Morse potential or the modified Buckingham potential. The harmonic-oscillator potential gives a reference to other (one-dimensional) calculations and at the same time offers an easy check for the numerical computations. It is clear that this potential is not expected to give good results for energy transfer exceeding a few eV's. The agreement between the one-dimensional harmonic oscillator and the experiment seems to be accidental as has already been pointed out. A more realistic potential for a diatomic molecule is the Morse potential, which allows the molecule to dissociate. It has, however, the disadvantage that the repulsive part of the potential is rather unphysical. This difficulty is circumvented when the modified Buckingham potential is applied as suggested by Linnett¹¹).

For one particular case (K^+-H_2) the three potentials are applied, so that we can compare their effect on the energy transfer. Finally the third potential is used to discuss some practical cases.

3. *The equations of motion.* The collision model is shown in fig. 1b. The initial conditions are such that the direction of the velocity of a is always pointing at the centre of the atom b of the molecule. The direction of the molecular internuclear axis with respect to the incident velocity is arbitrary and can be characterized by one single parameter, the angle ψ .

The Lagrangian for the three particles is

$$\begin{aligned} \tilde{L} = & \frac{1}{2}m_a\dot{r}_a^2 + \frac{1}{2}m_b\dot{r}_b^2 + \frac{1}{2}m_c\dot{r}_c^2 \\ & - V_{ab}(|r_a - r_b|) - V_{ac}(|r_a - r_c|) - V_{bc}(|r_b - r_c|), \end{aligned}$$

where r_i and \dot{r}_i ($i = a, b, c$) are the position and the velocity vector of the i th particle. The interaction between the projectile and the molecule is represented by an exponential potential, so that

$$V_{ab}(r) \equiv V_{ac}(r) = A \exp[-r/L].$$

For $V_{bc}(r)$ any of the three potentials mentioned above can be taken, and for the present be denoted by V .

We make the coordinate- and time-scale transformation

$$y = \lambda/L (r_c - r_b), \quad x = 1/L [(m_b r_b + m_c r_c)/(m_b + m_c) - r_a],$$

$$R = (m_a r_a + m_b r_b + m_c r_c)/M, \quad \tau = (k/\mu)^{1/2} t,$$

where

$$\lambda = m_c/(m_b + m_c), \quad M = m_a + m_b + m_c, \quad \mu = m_b m_c/(m_b + m_c)$$

and k is the force constant of the molecule. Introducing then the quantities

$$\mathcal{L} = \lambda^2 \tilde{L}/kL^2, \quad U = \lambda^2 V/kL^2, \quad \alpha = \lambda^2 A/kL^2$$

and

$$m = m_a m_c / M m_b,$$

the resulting lagrangian in the centre-of-mass system is

$$\begin{aligned} \mathcal{L} = & \frac{1}{2}m\dot{x}^2 + \frac{1}{2}\dot{y}^2 \\ & - \alpha \exp[-|x - y|] - \alpha \exp[-|x + y(1 - \lambda)/\lambda|] - U(y). \end{aligned}$$

The total energy of the system, ε , is now measured in units kL^2/λ^2 (λ^2). The dotted quantities are differentiated with respect to τ , which is the dimensionless time parameter, expressing the time in units of the vibration time of the molecule in its ground state.

The parameters of the intramolecular potentials are expressed in terms of the molecular constants D_e , r_e and ω_e , the dissociation energy, the internuclear distance and the vibrational frequency of the ground state, respectively.

The modified Buckingham potential,

$$V(r) = (a/r^{m'}) - b e^{-nr},$$

($a, b, m', n > 0$), has four parameters. The additional degree of freedom can be used to vary the steepness of the repulsive part of the potential, characterized by m' . In the present calculations m' has been given the value 3.

The equations of motion are given by the Euler-Lagrange equations and form four second-order coupled differential equations. They are solved by a standard Runge-Kutta numerical-integration procedure. The initial and final values of $|r_a - r_b|$ and $|r_a - r_c|$ must be chosen sufficiently large so that the interaction potential is very small. The constancy of the total energy along the trajectory was used as a reliability check for the energy transfer solutions. The vibrational and rotational energy of the diatomic molecule before the collision is neglected.

4. *Results.* For a fixed combination of particles ($K^+ - H_2$) the relative energy transfer (Q/E) and the laboratory scattering angle (θ) were calculated as functions of energy and molecular orientation. For small values of $r - r_e$ the shape of the Morse and modified Buckingham potential curve becomes equivalent to the harmonic-potential curve, which leads to the same results for the three potentials, when the impact energy is low. When the energy increases the harmonic potential gives different results in comparison with the Morse and the modified Buckingham potential. The latter two potentials give nearly equivalent results over the whole energy range and for all molecular orientations.

Only for (nearly) collinear configurations, where the repulsive part of the potential plays an important role, is the energy transfer for the modified Buckingham potential somewhat less effective. With the parameter m' the softness of the repulsive potential can be varied. The effect, however, of such a variation on the energy transfer is small. A general conclusion which is valid for all the applied potentials is that, in agreement with Kelly and Wolfsberg's calculations⁷), collinear collisions are very ineffective in transferring vibrational energy to the molecule as compared with collisions where the molecular axis is rotated slightly with respect to the incident direction.

The experimental data concern mostly energy transfer in collisions where the (heavy) incident particle is scattered in the forward direction in the laboratory frame. Therefore it is interesting to know which molecular orientations contribute to laboratory small-angle scattering. (Here and elsewhere in the paper the term small-angle scattering is used for scattering in the laboratory system over angles smaller than 0.5° , that being the maximum angular aperture of the apparatus⁸.) We conclude that there are two ranges of molecular orientations contributing to small-angle scattering; one where the molecule is oriented about the incident direction and the other perpendicular to it. This is illustrated by fig. 2. In the first

case the motion of the atom b, during the collision with incident atom a, is strongly disturbed by atom c *via* the repulsive part of the molecular potential, so that in this case both atoms are strongly involved in the collision. We propose to refer to this type of collision as a "molecular" collision. In the second case the motion of atom b is only weakly influenced by the presence of atom c, as a consequence of the soft attractive part of the molecular bond. This case, where atom c is not strongly involved in the collision, we propose to refer to as a "stripping" or "spectator" collision. These two cases are discussed separately:

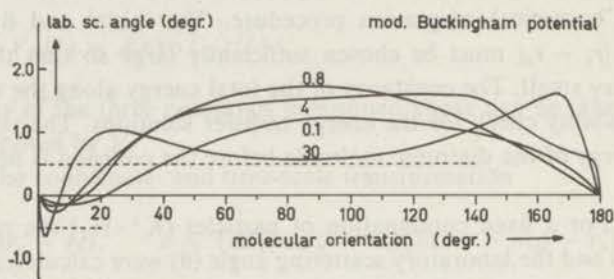


Fig. 2. Laboratory scattering angle (θ) versus molecular orientation (ψ) at a reduced energy $\epsilon = 0.1, 0.8, 4$ and 30 . The dashed lines represent the maximum angular aperture of the apparatus of ref. 8.

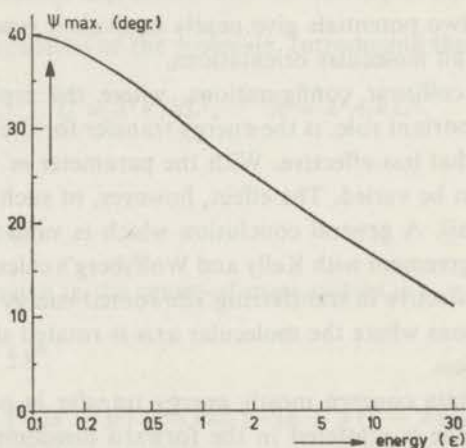


Fig. 3. Upper limit of the range of orientations of the molecule for which the incident particle is scattered within 0.5 deg as a function of the energy.

4.1. Molecular collision. At low energies this is the only type of collision where the incident particle is scattered in the forward direction (*cf.* fig. 2). It is observed that the range of orientations contributing to small-angle scattering

decreases for higher energies as shown in fig. 3. This explains the extinction of the first energy-loss peak with increasing energy. The corresponding average energy loss,

$$\langle Q/E \rangle = \int_0^{\psi_{\max}} Q/E(\psi) \sin \psi \, d\psi / \int_0^{\psi_{\max}} \sin \psi \, d\psi,$$

is plotted in fig. 5 as a function of energy together with the experimental data⁸). The upper limit of the integral, ψ_{\max} , is the molecular orientation for which a scattering angle of 0.5° is reached. It is observed that the calculated values below 20 eV overestimate the experimental values by about a factor of two. This error is one of the shortcomings of the model due to the fact that only zero impact-parameter collisions are considered.

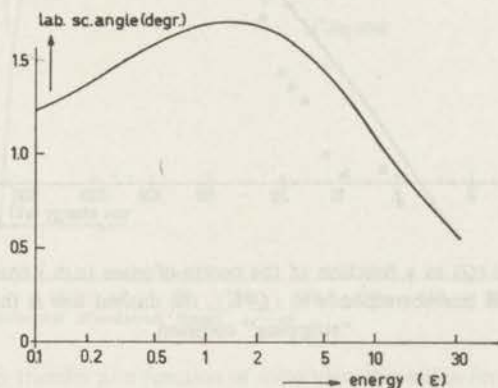


Fig. 4. Laboratory scattering angle as a function of the reduced energy when the molecule was initially oriented perpendicular to the incident direction.

4.2. Stripping collision. At low energies the scattering angle corresponding with a stripping collision is too large to be observed in the forward direction. At higher energies the scattering angle decreases for perpendicular orientations (*cf.* figs. 2 and 4). This explains the appearance of the second peak in ref. 8, at a somewhat higher energy (22 eV). The rapid increase in intensity of this peak is in agreement with the high statistical weight of perpendicular orientations. In fig. 5 the energy transfer for this type of collision is given as a function of energy and compared with experimentally obtained values. The relative energy loss (Q/E) tends to

$$[4m_a m_b m_c (m_a + m_b + m_c)] / [(m_a + m_b)^2 (m_b + m_c)^2],$$

in the case of vanishing molecular bond. Both theory and experiment show this behaviour (*cf.* fig. 5). We may conclude that this particular collision model gives

qualitatively a fair description of the observed data. The appearance of double energy-loss peaks is explained by considering different molecular orientations separately. In order to get better quantitative agreement at low energies a more sophisticated calculation should be made, including also nonzero impact-parameter collisions.

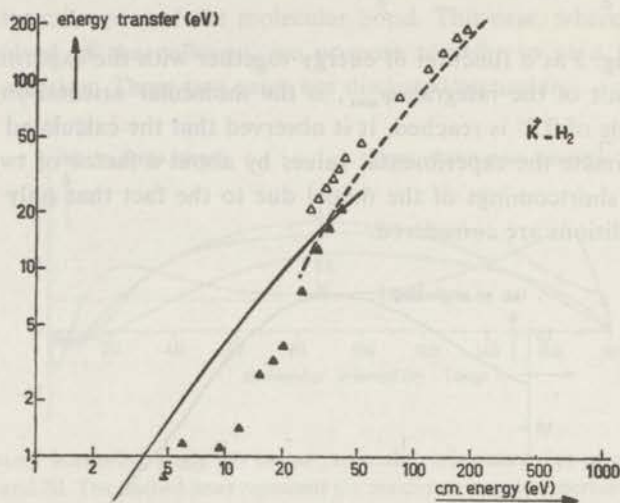


Fig. 5. Energy transfer (Q) as a function of the centre-of-mass (c.m.) energy (E). Δ , \blacktriangle experimental data⁸), the solid line corresponds to $\langle Q/E \rangle$, the dashed line is the energy transfer in a "stripping" collision.

Finally some practical cases are considered, all with an impact energy of 10 eV (c.m.s.).

4.2.1. K^+-H_2 , K^+-D_2 . For both combinations the small-angle scattering is limited to molecular orientations smaller than about 30° . The energy transfer for the combination K^+-H_2 is somewhat more effective. Q/E amounts to roughly 0.5 for both. This overestimates the experimental values by about a factor 2.

4.2.2. Na^+-H_2 , Na^0-H_2 . The energy transfer for Na^0-H_2 is less effective. The only difference between the ionic and the neutral collision occurs in the screening parameter L . For the neutral atom L is about 50% larger. This will in general reduce the energy transfer considerably, as is indeed observed by Dittner and Datz⁹). This result was also found by Cheng and Wolfsberg⁹), who did a three-dimensional calculation, using a Morse potential.

4.2.3. K^+-HD . Here an asymmetry is introduced in the molecule. This has the important consequence for our collision model that the energy transfer will be double-valued at each molecular orientation, depending on whether the collision will be head-on the H or D atom of the molecule. The energy-transfer difference

for a (high-energy) stripping collision is sufficiently large to observe experimentally. Experimental evidence was only available at about 700 eV c.m. energy for the combination $\text{Ar}^+ - \text{HD}^8$), where indeed two peaks are observed.

4.2.4. $\text{Li}^+ - \text{H}_2$. In fig. 6 it is shown that, with the exception of (nearly) collinear configurations, the energy-transfer ratio Q/E is somewhat less than one, while molecular orientations ranging from 20° to 40° contribute to scattering over angles smaller than 0.5° in the laboratory frame. The collision has in this case a stripping character for almost all molecular orientations, already at a rather low energy.

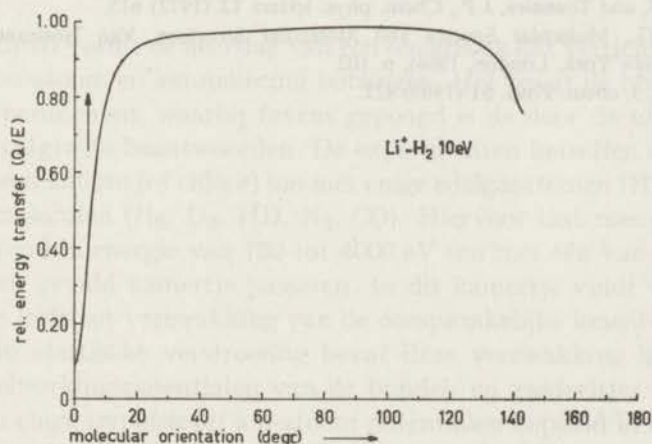


Fig. 6. Relative energy transfer as a function of molecular orientation for $\text{Li}^+ - \text{H}_2$ at 10 eV c.m. energy.

This is due to the small screening parameter L of the $\text{Li}^+ - \text{H}$ interatomic potentials. This explains possibly why Schöttler *et al.*¹⁰), who did some experiments in this field with Li^+ incident on H_2 , found only one peak corresponding with a stripping collision, the intensity of the other one already being too small to observe at these energies.

Acknowledgements. The authors are indebted to Drs. A. v.d. Meulen for his computational advice. This work is part of the research program of the Stichting voor Fundamenteel Onderzoek der Materie (Foundation for Fundamental Research on Matter) and was made possible by financial support from the Nederlandse Organisatie voor Zuiver-Wetenschappelijk Onderzoek (Netherlands Organization for the Advancement of Pure Research).

REFERENCES

- 1) Kelly, J.D. and Wolfsberg, M., J. chem. Phys. **44** (1965) 324.
- 2) Rapp, D. and Kassal, T., Chem. Rev. **69** (1969) 61.
- 3) Shin, K.H., Chem. Phys. Letters **7** (1970) 436.
- 4) Secrest, D. and Johnson, B.R., J. chem. Phys. **45** (1966) 4556.
- 5) Heidrich, F.E., Wilson, K.R. and Rapp, D., J. chem. Phys. **54** (1971) 3885.
- 6) Mahan, B.H., J. chem. Phys. **52** (1970) 5221.
- 7) Kelly, J.D. and Wolfsberg, M., J. chem. Phys. **53** (1970) 2967.
- 8) van Dop, H., Boerboom, A.J.H. and Los, J., Physica **54** (1971) 223.
- 9) Dittner, P.F. and Datz, S., J. chem. Phys. **54** (1971) 4228.
- 10) Schöttler, J. and Toennies, J.P., Chem. phys. letters **12** (1972) 615.
- 11) Herzberg, G., Molecular Spectra and Molecular Structure, Van Nostrand (Princeton, Toronto, New York, London, 1966), p. 102.
- 12) Secrest, D., J. chem. Phys. **51** (1969) 421.

SAMENVATTING

Dit proefschrift vormt de neerslag van een onderzoek dat verricht is op het gebied van ion-atoom en ion-molecuul botsingen. Het bevat de beschrijving van enige experimenten, waarbij tevens gepoogd is de door de uitkomsten opgeworpen vragen te beantwoorden. De experimenten betreffen de wisselwerking van een kalium (of chloor) ion met enige edelgasatomen (He, Ne, Ar, Kr, Xe) en moleculen (H_2 , D_2 , HD, N_2 , CO). Hiervoor laat men een ionenbundel variërend in energie van 150 tot 4000 eV een met één van bovengenoemde gasen gevuld kamertje passeren. In dit kamertje vindt verstrooiing plaats die leidt tot verzwakking van de oorspronkelijke ionenbundel. In het geval van elastische verstrooiing bevat deze verzwakking informatie over de wisselwerkingspotentialen van de bundel- en gasdeeltjes. Uit deze metingen zijn enige (repulsieve) ion-atoom potentialen bepaald in een interactie gebied variërend van ca. 1 tot 3 Å. Het is gebleken dat de wisselwerking in het algemeen een exponentieel karakter heeft in dit gebied. De relatieve contractie van het kalium-ion t.o.v. het chloor-ion is experimenteel waarneembaar. Vervolgens is een analoog experiment gedaan met enige moleculen. De wisselwerking tussen een individueel ion en een molecuul laat zich echter niet meer beschrijven met behulp van een bolsymmetrische potentiaal. De in dit experiment bepaalde potentialen zijn dan ook een gemiddelde over oriëntatie van de hoekafhankelijke ion-molecuul potentiaal. Voor hetero-nucleaire moleculen geeft de middeling over het hoekafhankelijke deel van de potentiaal een bijdrage aan de botsingsdoorsnede, die echter gezien de beperkte nauwkeurigheid van de metingen experimenteel niet verifieerbaar was.

Dit experiment heeft geleid tot een onderzoek naar de voorwaardenwaaronder de quantum mechanische beschrijving van de verstrooiing aan een potentiaal overgaat in de klassieke beschrijving, met name in het geval van een niet bolsymmetrische potentiaal. Uit deze correspondentie volgen enige relaties die een generalisering zijn van de relaties voor een bolsymmetrische potentiaal.

Door de in voorwaartse richting verstrooide ionen op energie te selecteren

was het mogelijk enige inelastische processen in botsingen met moleculen te bestuderen. Het voornaamste inelastische proces bleek vibratie-aanslag (of bij hogere energie dissociatie) van het molecuul te zijn. Op grond van de uitkomsten van deze metingen blijkt dat de beschrijving van vibratie aanslag door botsing met behulp van een één dimensionaal model weinig bevredigend is. De door de auteur uitgevoerde berekeningen aan een twee dimensionaal model voldoen beter aan de experimentele waarnemingen.

CURRICULUM VITAE

Teneinde te voldoen aan de wens van de faculteit der Wiskunde en Natuurwetenschappen volgt hier een kort overzicht van de studie van de promovendus.

In 1961 behaalde hij het eindexamen HBS-b 5-jarige cursus aan het Libanon-Lyceum te Rotterdam. Kort daarop volgde zijn inschrijving aan de Universiteit van Leiden, in de faculteit der Wiskunde en Natuurwetenschappen. In september 1965 legde hij het candidaatsexamen in de Wis- en Natuurkunde – met bijvak sterrenkunde – af, waarna hij in februari 1969 het doctoraalexamen in de Wis- en Natuurkunde – gemengde studierichting – wist te verwerven. Inmiddels was hij in mei 1968 in dienst getreden bij de Stichting F.O.M. als student assistent op het laboratorium voor Atoom- en Molecuulfysica te Amsterdam onder leiding van Professor dr. J. Kistemaker. Na zijn doctoraalexamen mocht hij zijn onderzoek op de afdeling van Dr. A. J. H. Boerboom als wetenschappelijk medewerker voortzetten. In de maanden juli en augustus 1971 bezocht hij de Quantum Chemistry Zomerschool te Uppsala geleid door Professor P. O. Löwdin.

The following is a list of the names of the persons who have been elected to the office of the President of the United States since the year 1789. The names are given in the order in which they were elected, and the year of their election is given in parentheses. The names are given in the order in which they were elected, and the year of their election is given in parentheses.

CURRICULUM VITAE

The following is a list of the names of the persons who have been elected to the office of the President of the United States since the year 1789. The names are given in the order in which they were elected, and the year of their election is given in parentheses. The names are given in the order in which they were elected, and the year of their election is given in parentheses.

The following is a list of the names of the persons who have been elected to the office of the President of the United States since the year 1789. The names are given in the order in which they were elected, and the year of their election is given in parentheses. The names are given in the order in which they were elected, and the year of their election is given in parentheses.

